

Review

Low-Temperature Electrochemical Oxidation of Methane into Alcohols

Adeel Mehmood¹, Sang Youn Chae^{1,2,*}  and Eun Duck Park^{1,3,*} 

¹ Department of Energy Systems Research, Ajou University, Suwon 16499, Republic of Korea; adeelmkhank007@ajou.ac.kr

² Institute of NT-IT Fusion Technology, Ajou University, Suwon 16499, Republic of Korea

³ Department of Chemical Engineering, Ajou University, Suwon 16499, Republic of Korea

* Correspondence: sychae@ajou.ac.kr (S.Y.C.); edpark@ajou.ac.kr (E.D.P.)

Abstract: The direct oxidation of methane to methanol is considered challenging due to the intrinsically low reactivity of the C–H bond of methane and the formation of a large number of unstable intermediates (methanol, formaldehyde, and formic acid) relative to the yield of methane. However, promising advances have recently been reported in this area based on the use of electrochemical systems that differ from traditional thermal catalysis. In this review, the recent advances in direct and indirect electrochemical methane conversion with homogeneous catalysts are reviewed and discussed, especially under low-temperature conditions. Finally, the limitations of the current electrochemical methane conversion technology and future research directions are discussed.

Keywords: methane; electrochemistry; methanol; electrocatalyst; selective oxidation

1. Introduction

Methane (CH₄) is a major component of various gas resources, including natural gas, associated gas, coalbed methane, shale gas, biogas, and gas hydrates [1]. Each gas resource possesses different reserves and compositions, but the total amount is considered sufficient to meet the current and foreseeable future needs of the energy and chemical industries [2,3]. Methane also exhibits the highest H/C ratio among hydrocarbons and relatively fewer impurities compared to coal and oil, thus making it an attractive feedstock for the production of energy and chemicals [4,5]. Moreover, methane is a major greenhouse gas along with CO₂, and therefore, its utilization and emission management are important [6–9]. Recently, the use of methane as a chemical feedstock has become more prominent as renewable energy has replaced traditional power plants that use fossil fuels, including methane. However, the inertness of methane has hindered its widespread use in the chemical industry.

Methane possesses a tetrahedral geometry characterized by high symmetry and low polarity. As methane exhibits the highest dissociation energy of the C–H bond (439.3 kJ mol^{−1}) among alkanes, activation of C–H bonds in methane has proved challenging [10–12]. Additionally, during the partial oxidation of methane, most intermediates (CH₃OH, HCHO, HCOOH, and C₂H₄) are less stable than methane itself, thus resulting in low yields of these intermediates under the harsh conditions used for methane activation [1,13,14]. Therefore, the current commercial methane conversion process is based on an indirect route using syngas, which is a mixture of CO and H₂. This is an energy-intensive process, and only large-scale plants are cost-competitive [15,16]. Numerous studies have been conducted using various thermal catalysts due to the advantages of direct methane conversion technology. However, the need for expensive oxidants, including H₂O₂ and N₂O, and low product yields remain challenges [17].

One potential alternative is the use of electrochemical systems to directly convert methane into value-added products. Electrocatalysis has exhibited some promise for this



Citation: Mehmood, A.; Chae, S.Y.; Park, E.D. Low-Temperature Electrochemical Oxidation of Methane into Alcohols. *Catalysts* **2024**, *14*, 58. <https://doi.org/10.3390/catal14010058>

Academic Editor: Junling Lu

Received: 25 December 2023

Revised: 6 January 2024

Accepted: 10 January 2024

Published: 12 January 2024



Copyright: © 2024 by the authors. Licensee MDPI, Basel, Switzerland. This article is an open access article distributed under the terms and conditions of the Creative Commons Attribution (CC BY) license (<https://creativecommons.org/licenses/by/4.0/>).

purpose compared to thermal catalysis [1,13,18]. Electrochemical processes can promote methane conversion at low temperatures (below 100 °C), as the chemical potential of the catalyst surface can be controlled [19–21]. This method also possesses the potential to avoid the use of strong and expensive oxidants such as N_2O and H_2O_2 , as well as the significant thermal energy demand associated with the activation of methane and/or regeneration of active sites. The driving force of CH_4 conversion can be controlled by changing the electrode potential, ultimately resulting in a non-equilibrium distribution of highly reactive metal centers and a faster reaction rate than thermal processes [22]. Mild reaction conditions prevent excessive methane oxidation [23]. Additionally, the electricity required for methane electrooxidation can be obtained from renewable energy sources such as sustainable solar and wind power [18,24]. Moreover, gas diffusion electrode-type reactors can be designed to operate at low overpotentials using efficient electrocatalysts, thus allowing them to selectively produce target chemicals using less electricity [25–28]. Due to their high degree of modularity, electrochemical devices are efficient and economically viable options for both small-scale applications and large-scale industries (Figure 1) [29].

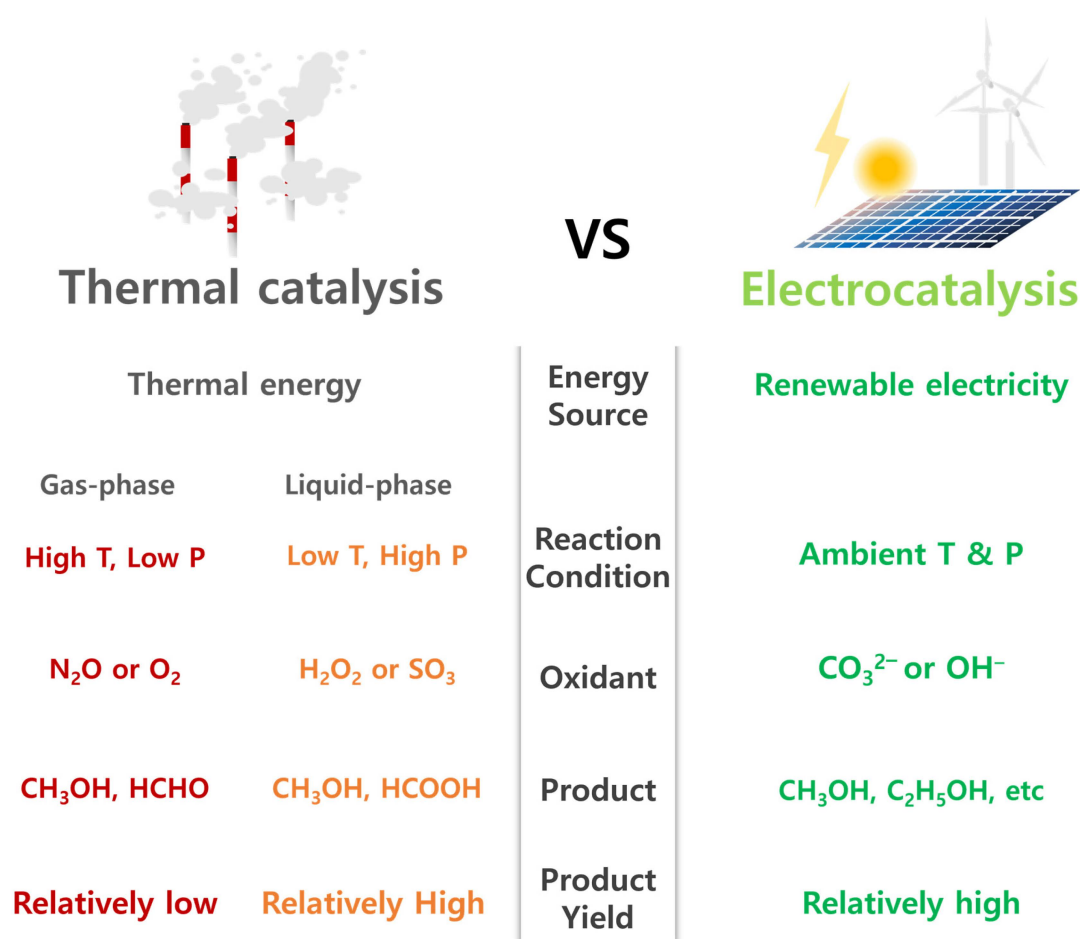


Figure 1. Thermal catalysis vs. electrocatalysis for selective oxidation of CH_4 .

In this review, we summarize the low-temperature electrochemical conversion of methane to high-value products (e.g., alcohol) using direct and indirect methods. We also discuss the research directions for the design of electrocatalysts with improved activity and selectivity. Finally, we discuss the issue of scaling up to increase the methane conversion.

2. Direct Electrochemical Conversion of Methane

Direct electrochemical methane conversion involves the activation of the C–H bond of methane with a reactive species produced by an electrocatalyst under an external bias.

These reactive species must be able to efficiently activate methane, but they are not sufficiently reactive to cause excessive oxidation of the intermediate so that a high yield of valuable products can be obtained [30]. The direct conversion of methane has been explored using various electrochemical systems. The simplest system consisted of a single-compartment cell with working and counter electrodes submerged in an aqueous electrolyte (Figure 2a). In other systems, proton exchange membrane (PEM) and anion exchange membrane (AEM) electrolysis are performed for methane conversion at the anode. The ion[−] exchange membrane separates the anode from the cathode and allows only selective ion transport. In AEM electrolysis, the charge carrier OH[−] carries charge through the AEM from the cathode to the anode, while in PEM electrolysis, the H⁺ charge carrier works by carrying charge from the anode to the cathode through PEM (Figure 2b,c). Table 1 lists the reactions and standard potentials associated with methane oxidation via electrolysis. These electrochemical systems can be classified into two categories based on the target product. One was for C₂₊ alcohols, including ethanol, acetone, and propanol, and the other was for methanol.

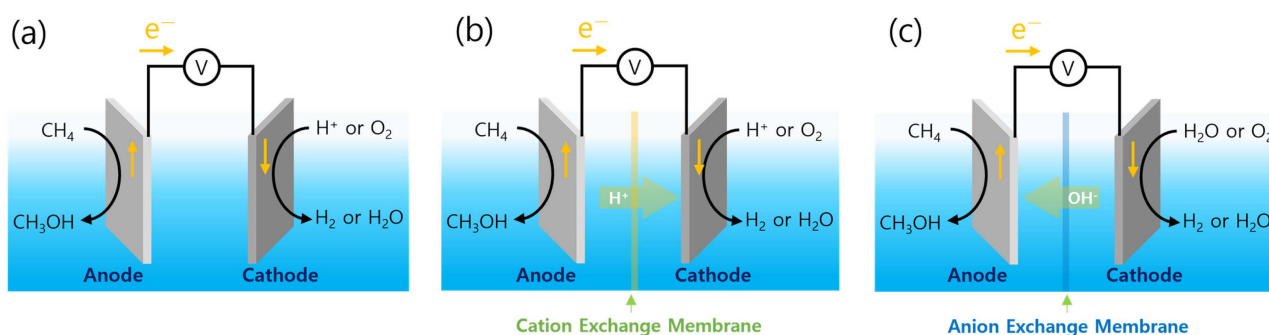


Figure 2. Direct electrochemical conversion of methane (a) in one-body electrolyte, (b) in separated electrolyte via cation (proton) exchange membrane, and (c) in separated electrolyte via anion exchange membrane.

Table 1. Electrochemical reactions for methane conversion in the membrane electrode assembly (MEA) [25].

Half-Cell Reactions	Proton Exchange Membrane	V vs. SHE
Anode	$\text{CH}_4 + \text{H}_2\text{O} \rightarrow \text{CH}_3\text{OH} + 2\text{H}^+ + 2\text{e}^-$	0.58
	$2\text{H}_2\text{O} \rightarrow \text{O}_2 + 4\text{H}^+ + 4\text{e}^-$	1.23
Cathode	$\text{O}_2 + 4\text{H}^+ + 4\text{e}^- \rightarrow 2\text{H}_2\text{O}$	1.23
	$2\text{H}^+ + 2\text{e}^- \rightarrow 2\text{H}_2$	0.00
Anion Exchange Membrane		
Anode	$\text{CH}_4 + 2\text{OH}^- \rightarrow \text{CH}_3\text{OH} + \text{H}_2\text{O} + 2\text{e}^-$	−0.18
	$4\text{OH}^- \rightarrow \text{O}_2 + 2\text{H}_2\text{O} + 4\text{e}^-$	−0.40
Cathode	$\text{O}_2 + 2\text{H}_2\text{O} + 4\text{e}^- \rightarrow 4\text{OH}^-$	−0.40
	$2\text{H}_2\text{O} + 2\text{e}^- \rightarrow \text{H}_2 + 2\text{OH}^-$	−0.83

2.1. Methane to C₂₊ Alcohols

Compared to thermal catalysis, the coupling of methyl radicals to form C₂₊ alcohols has been frequently reported, even at room temperature, in electrochemical systems. These can be further categorized according to the type of electrolyte used. Carbonate- or hydroxide-soluble electrolytes have been mainly studied, and there are also other electrolytes (polymer membrane electrolytes or gas-phase electrochemical reactions). The selection of an electrolyte significantly affects the electrochemical oxidation of CH₄ to CH₃OH. Carbonate electrolytes are attractive oxidizing agents due to their ability to provide a charged oxygen atom through the reaction ($\text{CO}_3^{2-} \leftrightarrow \text{CO}_2 + \text{O}^{2-}$) under mild conditions.

Methane can be effectively oxidized using a charged oxygen atom in the carbonate-soluble electrolyte at low temperatures and pressures. However, the carbonate-soluble electrolyte suffers from excessive CO₂ emission during electrochemical methane conversion, which can be overcome by recycling the CO₂ to CO₃²⁻ by regulating the electrolyte pH [31]. The electrocatalytic conversion of CH₄ in alkaline is more environmentally friendly [18]. The hydroxide ion is often used in the electrochemical oxidation of CH₄ as an alkaline medium, which not only acts as a base but also serves as an oxidizing agent. Unfortunately, OH⁻ ions have negligible oxidizing ability to abstract protons from the C–H bonds in CH₄, especially under mild conditions. This is the reason why CH₄ oxidation in hydroxide media does not show appreciable activity [32]. However, metal oxide catalysts reported for methane oxidation, e.g., NiO [33], Co₃O₄ [34], and NiCO₂O₄ [35], are more stable under alkaline conditions. In solid electrolyte conditions, ion conductivity, cell design, electrochemical stability, and the material's pH environment can strongly affect the overall cell performance.

2.1.1. Carbonate Electrolyte

Kaur et al. investigated the electrocatalytic properties of mesoporous rutile TiO₂ (r-TiO₂) and Pt/r-TiO₂ nanorods synthesized using a one-step hydrothermal method. They investigated the electrocatalytic interaction of CH₄ with a Na₂CO₃ electrolyte over Pt/r-TiO₂ nanorods. Pt nanoparticles (NPs) on r-TiO₂ enhanced the reactivity between CH₄ and •OH, thereby facilitating the production of methyl radicals (•CH₃). Subsequently, 50 and 36 μmol/g_{cat.} h of CH₃OH and C₂H₅OH were produced along with a small amount of propanol using Pt/r-TiO₂ at an applied potential of 1.5 V_{Ag/AgCl} [36].

Park et al. designed an electrochemical system employing a Co₃O₄-incorporated ZrO₂ nanotube as an electrocatalyst in HCO₃⁻ as a supporting electrolyte. The design of this system was based on the activation of CH₄ by oxygen vacancies on the Co₃O₄ surface, and the bicarbonate electrolyte acted as an active oxygen donor for CH₄ conversion [34,37]. They performed electrochemical anodization of zirconium foil to form a ZrO₂ nanotube powder with a high specific surface area that was decorated with Co₃O₄ NPs, ultimately leading to a reduced onset potential for the electrochemical activation of methane. After 12 h at 1.4–1.8 V_{RHE}, the final product contains 1-propanol and 2-propanol with 92% total selectivity, along with a small proportion of CH₃OH [34]. They demonstrated that the synthesis of these higher alcohols occurred through the coupling of •CH₃ and surface intermediates with delayed desorption from the catalyst surface [37]. The low selectivity for CH₃OH can be caused by the complexity of the oxygen species produced through carbonate oxidation at the anode, ultimately leading to similar results to previous study [38]. Similarly, Spinner et al. reported the low-temperature electrochemical conversion of methane to CH₃OH, HCHO, CO, and HCOO⁻ by CO₃²⁻ ions. The CO₃²⁻ ions were transferred through an ion-conducting electrolyte to a NiO/ZrO₂ anode, where the negative charge oxygen of CO₃²⁻ was suggested for methane oxidation. Figure 3 presents the mechanistic pathways for the formation of methanol, ethanol, and other products [33]. In another similar study, Omasta et al. demonstrated the role of zirconia in methane activation at low temperatures in carbonate cells, in which carbonate ions provide active oxygen, unlike hydroxide-based cells, where NiOOH itself acts as the oxygen donor [39]. Even in a bilayer catalyst system consisting of NiOOH and an Mn porphyrin mediator, a cascade of O* occurs for CH₄ oxidation at ambient temperature. The methanol and formate were generated at 10.9 and 23.6% Faraday efficiency (FE), respectively, at 1.05 V_{SHE}, where the overoxidation to CO₂ was suppressed [40].

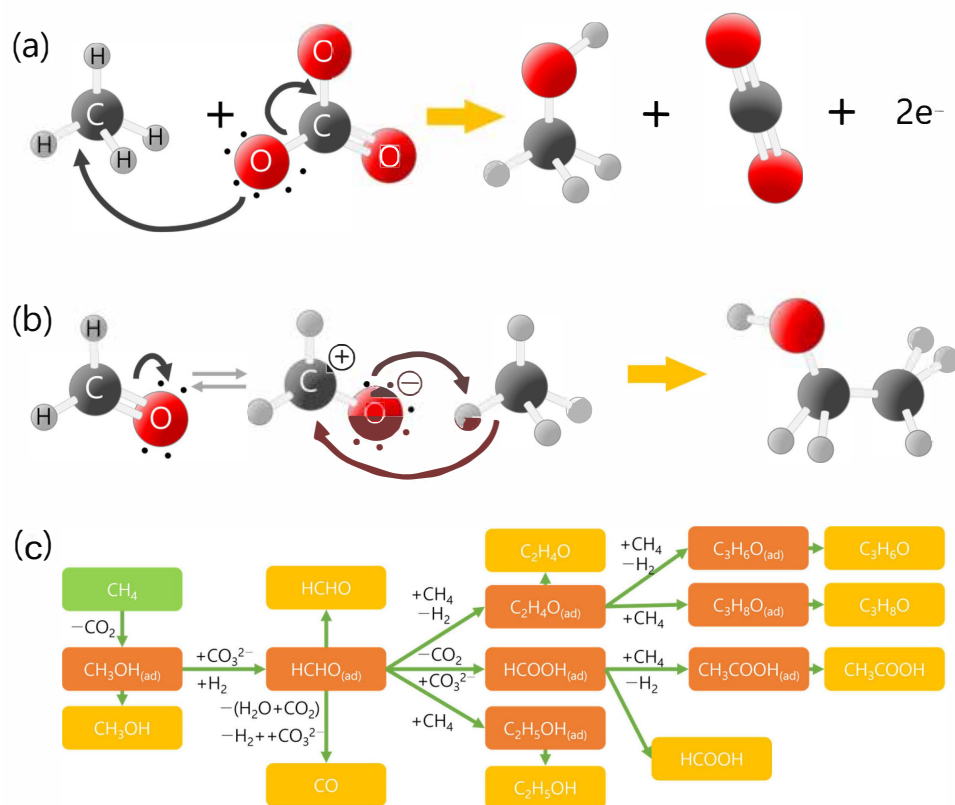


Figure 3. (a) Reaction mechanism of methane conversion via carbonate ions. (b) Formation of the C-C bond in ethanol. (c) Reaction pathways for methane activation via carbonate ions [33]. Copyright 2013, IOPscience.

Similarly, Xu et al. performed the electrochemical conversion of methane to liquid products at room temperature. A capsule-like ZrO₂/CuO_x bimetallic electrocatalyst was synthesized using a hydrothermal method. The high methane conversion activity of the bimetallic catalyst can be attributed to the synergistic interaction between ZrO₂ and CuO_x, which produces a unique electron transport route for enhancing electrochemical activity. DFT calculations indicated that ZrO₂-supported Cu₂O(111) exhibited an enhanced charge distribution, and this increased CH₄ dissociation and established a rapid electron transfer network. Considering these advantages, ZrO₂/CuO_x produced 1-propanol and 2-propanol as the primary products after 18 h [41]. Luo et al. demonstrated the electrocatalytic conversion of CH₄ to acetic acid over ZnO nanosheets in a bicarbonate electrolyte. The ZnO exhibited 75.5% FE, accompanied by 85% selectivity towards acetic acid at 1.3 V_{RHE}. The DFT estimation confirms that the strong bonding between adjacent Zn and O atoms lowers the reaction energy of the CH₃* + COOH* → CH₃*-COOH* step. A mechanistic investigation revealed that HCO₃⁻ was the reactive oxidative species that provided COOH during electrocatalytic methane oxidation [42].

Sumo et al. developed electrocatalysts by exploiting single Cu and Rh atoms dispersed in NH₄BF₄-modified alumina for the selective and direct oxidation of methane to C₂ products such as acetic acid and ethanol at ambient temperature. The alumina-supported single-atom catalyst possessed many Brønsted acid sites that play an important role by directly inserting CO into reaction intermediates. The Rh-based electrocatalyst obtained 95% current efficiency for acetic acid within 40 min, while the Cu-based electrocatalyst obtained 90% current efficiency for acetic acid after 120 min at 2.0 V_{Pt} with high yields of 33.57 and 33.57 μmol h⁻¹ cm⁻², respectively [43].

Kim et al. designed a shell/core-structured electrocatalyst consisting of NiO/ZnO nanorods for high CH₄ electrochemical conversion that was based on the 1D morphology of the nanorods and the built-in potential at the NiO/ZnO interface that allows fast charge

transfer. The conversion of CH_4 can be optimized by controlling the length of the nanorod catalyst, as presented in Figure 4a–e. Regarding the 600 nm long NiO/ZnO nanorod, FE, selectivity, and conversion values were recorded as 61%, 81%, and $1084 \mu\text{mol g}_{\text{NiO}}^{-1} \text{h}^{-1}$, respectively, at $1.5 V_{\text{Pt}}$. Mechanistic studies revealed that the ethanol production pathway includes the formation of active oxygen species by dissociative adsorption of the CO_3^{2-} oxidant, CH_4 activation for methanol formation, and coupling of CH_4 and deprotonated methanol (Figure 4f). Furthermore, the ethanol yield was improved by increasing the methanol solubility using sulfolane as a cosolvent and by in situ generation of the CO_3^{2-} oxidant [44].

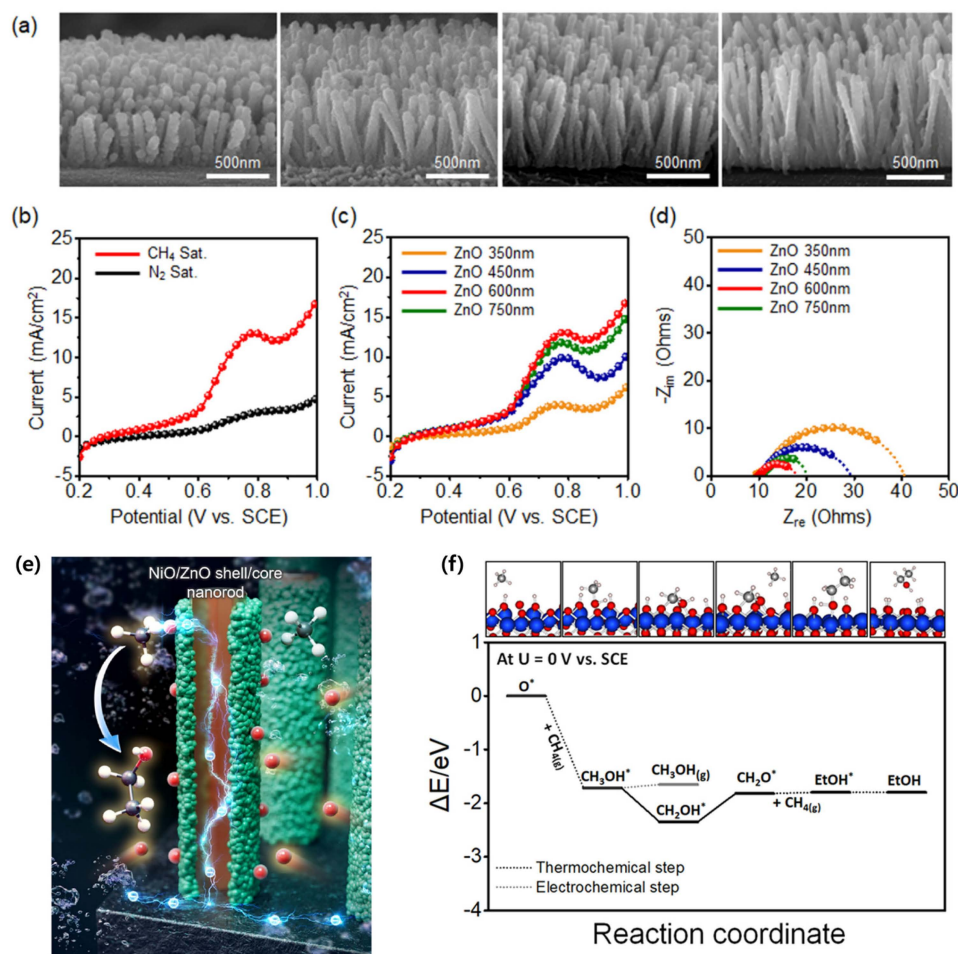


Figure 4. (a) SEM images of NiO/ZnO nanorods. (b) Polarization curves for NiO/ZnO nanorod catalysts with N_2 - and CH_4 -purged electrolytes. (c) LSV and (d) EIS spectra for the NiO/ZnO nanorod. (e) electrochemical methane conversion over the NiO/ZnO shell/core nanorod. (f) Energy diagram of the reaction coordinate for methane–ethanol conversion [44]. Copyright 2023, Elsevier.

2.1.2. Alkaline Electrolyte

Sun et al. demonstrated that a NiO/Ni interface exhibited significant activity for the electrooxidation of CH_4 , particularly with regard to the production of ethanol (Figure 5). The NiO/Ni interfacial catalyst attained 85–89% FE in ethanol at an applied potential of $1.40 V_{\text{RHE}}$. The increase in the peak current indicated the oxidation of Ni^{II} to Ni^{III} in the presence of CH_4 in the linear sweep voltammetry (LSV) polarization curves, and this further confirmed the high potential of the NiO/Ni interface for CH_4 activation. DFT calculations confirmed the effective activation of C–H bonds on the Ni(200)/Ni(111) interface that resulted in the non-oxidative coupling of C–C bonds, thus leading to the highly selective production of ethanol from the electrooxidation of CH_4 [45,46].

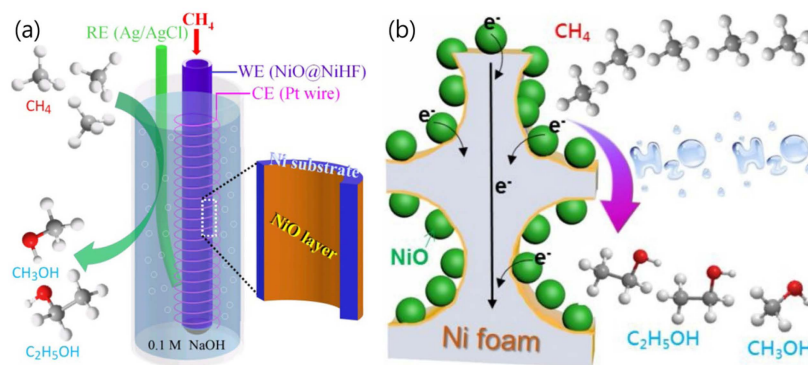


Figure 5. Electrochemical oxidation of CH_4 on (a) Ni/NiO hollow fibers and (b) a NiO/Ni foam anode [45,46]. Copyright 2020, Elsevier.

Xie et al. developed Rh/ZnO nanosheets for the electrochemical conversion of CH_4 into ethanol. Uniformly distributed Rh NPs were responsible for methane absorption, whereas ZnO provided excess active oxygen species for CH_4 activation. Rh/ZnO nanosheets exhibited 85%, 22.5%, and $789 \mu\text{mol}_{\text{cat}}^{-1} \text{h}^{-1}$ values for selectivity, FE, and conversion, respectively, towards ethanol at $2.2 V_{\text{RHE}}$ in a 0.1 M KOH solution [47].

Kim et al. performed oxygen evolution reaction (OER)-assisted electrochemical CH_4 oxidation at low temperatures using Fe–N–C single atom catalysts (SACs) to achieve high conversion and FE. A high FE for methane oxidation was obtained by employing the Fe single-atom catalyst, and this enabled the formation of OOH^* , which is a potentially limiting step in the OER, thus allowing the maintenance of a stable O^* intermediate (Figure 6). The O^* intermediate spontaneously activated CH_4 to form methanol, which then underwent deprotonation and was coupled with CH_4 to form ethanol. Fe–N–C SACs exhibited an ethanol selectivity of 85%, FE of 68%, and ethanol production rate of $4668 \mu\text{mol}_{\text{cat}}^{-1} \text{h}^{-1}$, respectively, at $1.6 V_{\text{RHE}}$. The authors also demonstrated the methane conversion in direct diffusion flow cells for rapid mass transfer, ultimately achieving an $11,480 \mu\text{mol}_{\text{cat}}^{-1} \text{h}^{-1}$ ethanol production rate [48].

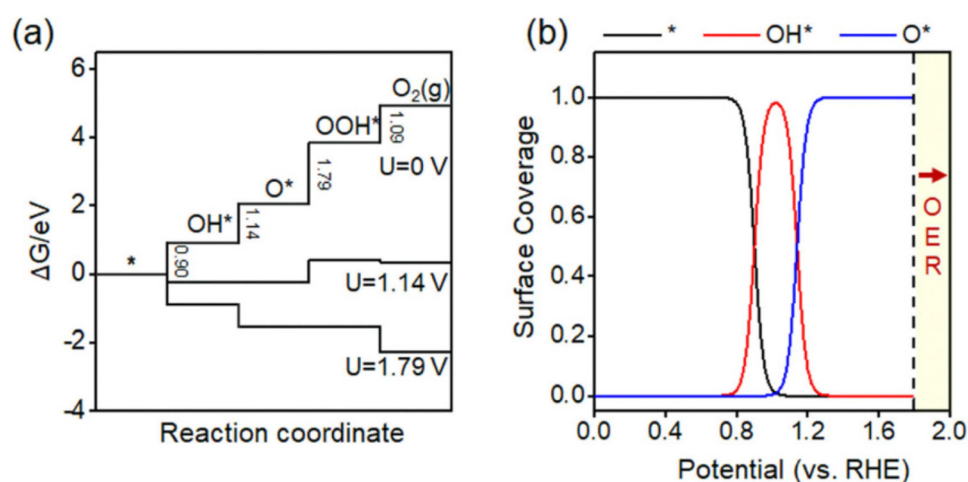


Figure 6. (a) The free energy diagram for the OER on Fe–N–C SACs. (b) The surface coverage of OER intermediates on Fe–N–C catalysts [48]. Copyright 2023, Royal Society of Chemistry.

2.1.3. Other Electrolytes

Ramos et al. utilized a proton-exchange membrane fuel cell as a single-stage solid electrolyte reactor (SER-FC) to transform methane into C_2 and C_3 products under mild conditions. The Pd/C electrocatalyst was synthesized using the sodium borohydride reduction technique, and this resulted in a cubic palladium crystal structure with a face-centered arrangement and an average nanoparticle diameter of approximately 6.4 nm. The

Pd catalyst activates water molecules, subsequently leading to the formation of methyl radicals due to the strong affinity of Pd for CH_4 . Figure 7 presents the reaction pathways in which non-oxygenated radicals such as $\bullet\text{CH}_3$ are formed at the propagation stage of the radical reaction under mild conditions, thus confirming the formation of C_2 and C_3 compounds such as C_2H_6 , C_3H_8 , $\text{C}_2\text{H}_5\text{OH}$, acetaldehyde, and acetic acid [49].

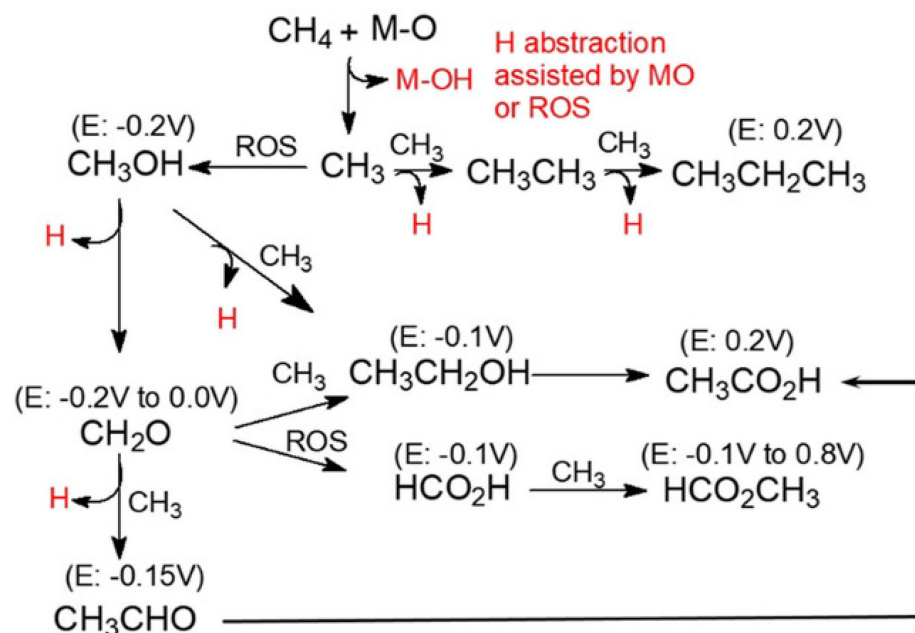


Figure 7. Proposed reaction pathways for partial oxidation of methane. The reaction pathways show the formation of C_2 and C_3 compounds via non-oxygenated radicals in the potential range of -0.2 – 0.8 V under mild conditions [49]. Copyright 2020, Wiley.

Hibino et al. also examined the individual production of CH_3OH and ethane from CH_4 using a thermo-electrochemical cell in a gas flow setup that operated within a temperature range of 150 to 200 °C. The direct oxidation of methane occurs at an anode consisting of Pt and Fe particles. The authors reported that methanol was synthesized by activation of water vapor to produce active oxygen species ($\text{H}_2\text{O} \rightarrow \text{O}^* + 2\text{H}^+ + 2\text{e}^-$; $\text{CH}_4 + \text{O}^* \rightarrow \text{CH}_3\text{OH}$), while ethane was synthesized via the dimerization of $\bullet\text{CH}_3$ radicals ($2\text{CH}_4 \rightarrow 2\bullet\text{CH}_3 + 2\text{H}^+ + 2\text{e}^-$; $2\bullet\text{CH}_3 \rightarrow \text{C}_2\text{H}_6$) [50].

Li et al. synthesized ultrathin WO_3 nanosheets with high oxygen vacancies for high conversion of CH_4 to ethanol. The oxygen vacancy facilitates the electrocatalytic activity and ethanol selectivity for CH_4 conversion by enabling the activation of C–H and coupling of the C–C bond. The WO_3 nanosheets outperform previous results by achieving a high ethanol selectivity of 99.4%, an FE of 50.7%, and a production rate of $125,090 \mu\text{mol}_{\text{cat}}^{-1} \text{h}^{-1}$ at $1.2 \text{ V}_{\text{RHE}}$ after 8 h of operation [51].

The performance of the electrochemical cell is significantly affected by the choice of an electrolyte, which influences the ion conductivity of the electrode material, surface reactivity, and stability. In alkaline media, the catalyst surface is oxidized via an electrolyte, resulting in electronic rearrangement, which generates lattice oxygen species for methane oxidation. In carbonate media, the methane is effectively oxidized via charged oxygen atoms, resulting in a lowered reaction barrier and accelerated kinetics for the methane oxidation reaction. Moreover, the utilization of a suitable electrolyte for a specific system can also affect the selectivity and yield of the desired product.

2.2. Methane to Methanol

Santos et al. synthesized a Pd–Ni electrocatalyst via NaBH_4 reduction. The PdNi catalyst was studied as an anodic material in alkaline direct methane fuel cells (ADMEFCs),

and the effect of the Ni content in the electrocatalyst on the methanol selectivity and fuel cell performance was investigated. It was observed that an increase in Ni content increased the power generation ability of the fuel cell. However, this system causes the over-oxidation of methanol due to the high water activation properties of NiO_x [52]. Considering the CH_4 activation properties of Ni-based catalysts, Surmo et al. designed a novel $\text{NiO-V}_2\text{O}_5/\text{Rh}$ electrocatalyst in which Rh was dispersed on a mixed-metallic oxide composite. The novel composite exhibited methanol productivity of $650 \mu\text{mol g}^{-1} \text{h}^{-1}$ with an FE of 91% and a selectivity of 98%. The uniformly distributed Rh NPs on the NiO matrix adsorbed CH_4 , whereas V_2O_5 provided active oxygen species for CH_4 activation, resulting in excellent catalytic performance [53]. Similarly, Godoi et al. utilized $\text{Pd}_x\text{Cu}_y/\text{C}$ catalyst combinations for the partial oxidation of CH_4 under moderate conditions using an alkaline fuel cell-type solid electrolyte reactor. The $\text{Pd}_{90}\text{Cu}_{10}/\text{C}$ and $\text{Pd}_{50}\text{Cu}_{50}/\text{C}$ electrocatalysts effectively activated H_2O and provided adequate carbophilic sites for CH_4 oxidation, thus resulting in high methane conversion to methanol and energy generation. Furthermore, the analysis revealed the existence of dimethyl ether and methyl formate, along with methanol [54].

Electrochemical methane conversion is significantly affected by water, as both processes compete at the anode surface. Water oxidation improves methane oxidation by forming active oxygen species. Arnarson et al. reported that the presence of active oxygen species facilitated hydrogen abstraction and improved methane conversion. The DFT results for monolayer MXenes and rutile transition-metal oxides indicated that the catalyst for which water oxidation is a bottleneck process exhibited the least tendency towards CH_4 oxidation. The materials on the left side of the volcano plot (Figure 8a) easily form adsorbed oxygen (O^*), thus making them suitable for methane oxidation. Considering the availability of O^* , they calculated the energy barrier for CH_3OH formation that decreased with increasing applied potential and ultimately resulted in an increase in the CH_3OH formation rate (Figure 8b). Additionally, the rate of CH_3OH formation versus the OER was studied as a function of the O^* binding energy. Figure 8c indicates that a high electrode potential facilitates the OER, ultimately resulting in the formation of abundant active sites on the electrode surface. Consequently, O_2 was the major product, and methanol productivity decreased. Although the OER provides active oxygen species, it also competes for methane conversion at high potentials [20].

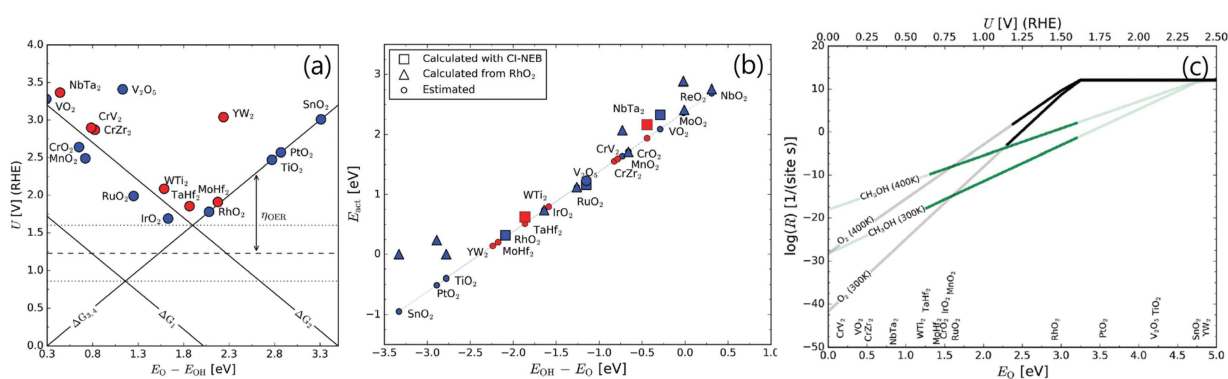


Figure 8. (a) Activity volcano plot of the OER for metal oxides (blue) and Mxenes (red). (b) Plot of methane activation energy versus the descriptor $E_{\text{OH}} - E_{\text{O}}$. (c) The reaction rates for the OER (black line) and methane oxidation (green line) versus E_{O} and U at different temperatures [20]. Copyright 2018, Royal Society of Chemistry.

Hsieh et al. also supported the involvement of O^* generated during the OER on an N-doped graphene material for methanol formation. Density functional theory (DFT) calculations indicated that the nitrogen atom in the vicinity of the active site stabilizes O^* for C–H bond activation. The presence of active oxygen (O^*) on the N-doped graphene led to a consistent electrode potential of 1.10 V_{SHE} . Consequently, compared to O^* -free N-doped graphene, active oxygen reduces the kinetic barrier energy of the rate-determining

step (C–H bond activation) by 0.82 eV. This indicates the significant role of the anodic potential in the O* reactivity towards methanol formation. The activation of the C–H bond initiated by hydrogen transfer, coupled with the excitation of one electron from the O* lone pair to the surface π orbital, increased the radical character of O* for transferring hydrogen [55]. Similarly, Kang et al. provided important information for understanding the relationship between the stability of active oxygen species, C–H bond activation, and the selectivity of oxygenates. The O-terminated anode surface was predominant over the OH-terminated and metal-terminated surfaces under an applied potential. O* can accumulate on the surface of the catalysts when the lower limit of the electrochemical potential for O* formation is less than that of O*. Figure 9a indicates that the MXenes in the right leg of the volcano plot are suitable for CH₄ oxidation, whereas those in the left leg favor OER. MXenes with a high proton affinity tend to stimulate the activation of the C–H bond, as indicated by the change in $\Delta E_{a,TS}$ (C–H bond activation) for the $\Delta E_{OH^*} - \Delta E_{O^*}$ (affinity energy of proton) that is presented in Figure 9b. In comparison to single-metal MXenes, bimetallic MXenes such as TaHf₂C₂O₂ and CrHf₂C₂O₂ can effectively perform CH₄ conversion due to their low energy barriers for C–H activation. In the case of TaHfC₂O₂, the formation of a relatively stable intermediate species depends on the applied potential for TaHfC₂O₂. (Figure 9c). Additionally, TaHf₂C₂O₂ favors the formation of oxygenates over hydrocarbons. The high tendency towards oxygenates can be attributed to the Hf–O bond being stronger than the Hf–C bond due to the small number of electrons in Hf (5d²) of TaHf₂C₂O₂ (Figure 9d). Previous studies have reported that the formation of hydrocarbons, CO, and CO₂ on metallic Pt can be explained by strong Pt and C interactions. As presented in Figure 9e, the number of electrons in the antibonding orbital of Pt–C was lower than that in Pt–O [56].

On transition metal oxides, electrochemical methane oxidation occurs via the physical adsorption of CH₄, which is followed by C–H bond activation. Upon physical adsorption, the tetrahedral symmetry of CH₄ was transformed into a distorted symmetry (D_{2d}), thus increasing the H–C–H bond to 120°. Therefore, the binding energy of CH₄ increases linearly with the Madelung potential. Active catalysts such as TiO₂, IrO₂, PbO₂, and PtO₂ possess high CH₄ binding energy (>0.23 V) and low Madelung potential (<–40 V). Based on the DFT profile, active catalysts such as TiO₂, IrO₂, PbO₂, and PtO₂ that exhibit higher adsorption energy of O* are capable of creating more reactive M–O sites and thus lowering the methane activation barrier [57].

Su et al. performed methane conversion using LaCo_{0.5}Fe_{0.5}O₃ as an anodic catalyst in a [BMIM]BF₄ ionic liquid with low water content as the supporting electrolyte. Trace water provided active oxygen species via water oxidation on the LaCo_{0.5}Fe_{0.5}O₃ surface. The extent of the CH₄ conversion depends on the generation of O*. The LaCo_{0.5}Fe_{0.5}O₃ electrocatalyst attained a methanol production rate of 93 $\mu\text{mol g}_{\text{cat}}^{-1} \text{h}^{-1}$ with 59% FE in an ionic liquid with 2.0 mol L^{–1} water content at 1.0 V_{Ag/AgCl} [58]. Another heterogeneous catalyst, Co_{0.6}Ni_{0.4}Fe₂O₄ loaded onto N-doped carbon nanocubes, exhibited high methane oxidation activity. The Co_{0.6}Ni_{0.4}Fe₂O₄-N/C produced methanol at a rate of 1925.4 mmol g_{cat.}^{–1} h^{–1} with 82.8% selectivity at 0.8 V_{Ag/AgCl}. The strong trimetal–carbon electronic interaction and high lattice oxygen/oxygen vacancy ratio of the Co_{0.6}Ni_{0.4}Fe₂O₄-N/C nanocubes are responsible for their robust catalytic performance [59].

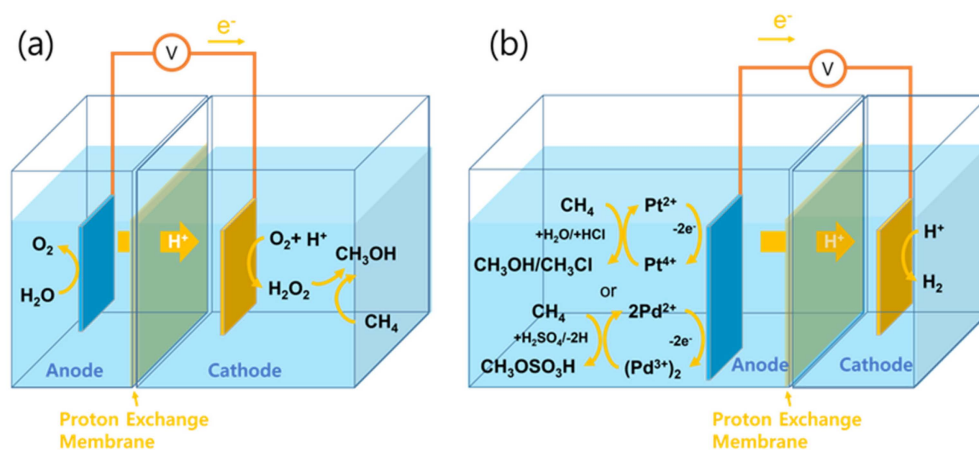
Shen et al. electrochemically deposited various thin-film transition metal (oxy) hydroxide electrocatalysts for the partial oxidation of methane. Among the various catalysts, CoO_x has been used as a prototypical CH₄ partial oxidation electrocatalyst. The effects of film thickness, overpotential, temperature, and electrochemical cell hydrodynamics on activity and methanol selectivity were optimized. The high thickness of the film provided a longer pathway for methanol on the catalyst surface, ultimately resulting in over-oxidation. Methanol was favorably produced at medium overpotentials ranging from 0.86 to 1.06 V_{SHE}. DFT analysis revealed that fully hydroxylated CoOOH provided a favorable thermodynamic pathway for methane activation and desorption. High temperatures result in low selectivity due to the high rate of thermal steps in CH₄ activation and CH₃OH overoxida-

Table 2. Summary of current state-of-the-art systems for electrochemical transformation of methane into chemicals.

Electrocatalyst	Temperature (°C)	Product	Potential (V)	Electrolyte	FE (%)	Yield (mmol g ⁻¹ h ⁻¹)	Selectivity (%)	Ref
NiO/Ni	RT	CH ₃ CH ₂ OH	1.40 vs. RHE	NaOH	89	2.5 × 10 ⁻²	87	[45]
Co ₃ O ₄ /ZrO ₂	RT	CH ₃ CH ₂ CH ₂ OH, CH ₃ CH(OH)CH ₃	1.6 vs. RHE	Na ₂ CO ₃	---	2.4	92	[37]
NiCo ₂ O ₄ /ZrO ₂	RT	CH ₃ CH ₂ CH ₂ OH, CH ₃ CH(OH)CH ₃	2.0 vs. Pt	Na ₂ CO ₃	---	1.2	---	[35]
0.6% Rh/ZnO	RT	CH ₃ CH ₂ OH	1.4 vs. RHE	KOH	23	0.79	85	[47]
CuO/CeO ₂	RT	CH ₃ OH	0.8 vs. SCE	Na ₂ CO ₃	---	0.75	79	[61]
Rh/NiO/V ₂ O ₅	100	CH ₃ OH	0.7 vs. RHE	Nafion	91	6.5 × 10 ²	98	[53]
Pt(IV)	130	CH ₃ OH	0.68 vs. SHE	NaCl, H ₂ SO ₄	100	2.9 × 10 ⁻⁴	70	[62]
NiO/Ni	RT	CH ₃ OH, CH ₃ CH ₂ OH	1.46 vs. SHE	NaOH	54, 85	---	78, 95	[46]
NiO/ZrO ₂	40	CH ₃ OH, HCHO, HCOOH, C ₂ H ₅ OH, CH ₃ COOH, C ₃ H ₈ O, C ₃ H ₆ O	2.0 vs. Cathode	Na ₂ CO ₃	---	---	HCHO: 44	[33]
TiO ₂ /RuO ₂ /V ₂ O ₅	RT	CH ₃ OH, HCHO, HCOOH	2.0 vs. SCE	Na ₂ SO ₄	57	---	CH ₃ OH: 97.7	[63]
ZrO ₂ /Co ₃ O ₄	RT	CH ₃ CH ₂ CH ₂ OH, (CH ₃) ₂ CHOH, CH ₃ CHO	2.0 vs. Pt	Na ₂ CO ₃	>100	---	>60	[34]

3. Indirect Electrochemical Conversion of Methane

Indirect electrochemical methane conversion involves electrochemical systems in which methane is not directly converted to methanol but to stable intermediates such as methane bisulfate and methyl chloride [22,64]. As they are more stable than methanol, they allow for efficient methane conversion with high product selectivity. Subsequently, hydrolysis can further convert these into methanol (Figure 10) [65].

**Figure 10.** Schematic diagram of indirect electrochemical conversion of methane. (a) Indirect oxidation in catholyte and (b) indirect oxidation in anolyte [14,22,62].

This process is based on homogeneous methane activation with highly active species such as radicals. Electrochemistry focuses on the generation of these radicals that convert CH₄ to CH₃OH or to its derivatives that can easily be converted to CH₃OH. The origins of this strategy can be traced back to the late 1980s and the early 1990s. These studies focus on the formation of HO• using the Fenton process [64], the generation of Cl• through photochemical reactions [66] in a complex system, and the formation of O₂^{•-} radicals in alkaline media for methane activation [67]. The mechanism of methane activation is based on a radical chain reaction that results in the formation of more than one product.

Although methanol is produced using these strategies, the selectivity and current efficiency are insufficient for scaled-up applications [64,67].

Inspired by this approach, electrochemistry can overcome some of the limitations of typical homogeneous catalytic systems [22]. Typically, transition-metal complexes are used with an external agent (usually a co-catalyst that can reoxidize the complex) for methane activation under ambient conditions [68]. The identification of a suitable co-catalyst with a higher redox potential than that of the catalyst is a significant challenge in homogeneous catalysis [22,68]. The redox potential of a co-catalyst is directly related to the number of catalytic cycles, where a higher redox potential is associated with a greater number of catalytic cycles. Therefore, the use of electrodes as co-catalysts is emerging as an attractive alternative for providing the potential difference required to promote catalyst regeneration [39,67,69].

Surendranath et al. selectively oxidized CH_4 to CH_3OH using an electrochemically assisted homogeneous catalyst [22]. Initially, they reported the conversion of CH_4 into two methanol derivatives, methyl bisulfate ($\text{CH}_3\text{OSO}_3\text{H}$) and methanesulfonic acid ($\text{CH}_3\text{SO}_3\text{H}$), using PdSO_4 at mild temperatures in a concentrated H_2SO_4 solution (Figure 11a) [22,70]. The system exhibited remarkable catalytic activity that was 5000-fold higher than that of an unassisted homogeneous catalyst system [22]. Similarly, Deng et al. employed vanadium (V) oxo dimer as a catalyst for CH_4 conversion to $\text{CH}_3\text{OSO}_3\text{H}$ with 90% FE under ambient conditions [69]. Other catalytic systems advanced one step further and produced methanol as the final product [62,71]. Inspired by the homogeneous catalysis activity with Pt complexes [72,73], Kim et al. utilized PtCl_4^{2-} and PtCl_6^{2-} as catalysts, resulting in methanol production with 70% selectivity at mild conditions [62]. Significant progress has been achieved in nonaqueous environments [71]. The system demonstrated the potential of the Rh complex as a catalyst for selective methanol production by controlling the O_2 concentration along the Si nanowire electrodes under ambient conditions. However, the complexity of the catalytic system restricts methane conversion (Figure 11b) [71].

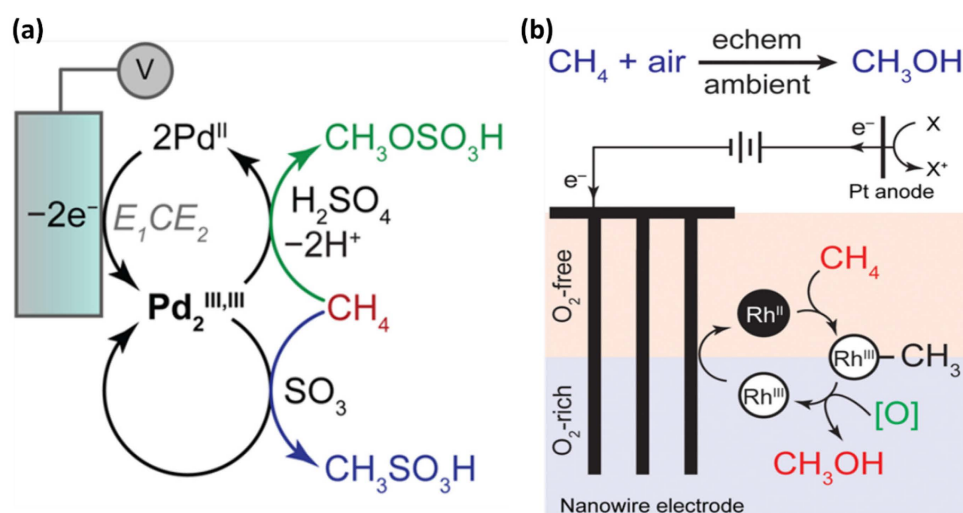


Figure 11. (a) Mechanism for electrochemical methane functionalization via a $\text{Pd}_2^{\text{III,III}}$ intermediate [22]. Copyright 2017, American Chemical Society. (b) Electrochemical methane functionalization catalyzed via an Rh-based catalyst in nonaqueous media and Si nanowires as electrodes [71]. Copyright 2019, American Chemical Society.

This electrochemically assisted homogeneous catalytic system exploits several possibilities for the highly selective conversion of methane to methanol. The integration of electrochemical and heterogeneous catalysis reduced the potential for OER and oxygen reduction reactions (ORR), thus allowing the production of methanol without overoxidation. However, it is important to note that this also possesses limitations. Specifically, effective electron transfer from the electrode to the catalyst must occur to regenerate the catalyst and

continue the conversion of methane to methanol [69]. Additionally, it is important to use a suitable catalyst with a metal center that promotes rapid electron transfer to avoid a high overpotential during catalyst regeneration [22].

Zheng et al. performed the electrochemical conversion of CH_4 to CH_3Cl using $^*\text{Cl}$ reactive species that were generated electrochemically on cobalt–nickel spinels. The CoNi_2O_x efficiently facilitated methane conversion in seawater, with an outstanding productivity of $364 \text{ mmol g}^{-1} \text{ h}^{-1}$ at 2.3 V. The electrochemically generated $^*\text{Cl}$ was stabilized by Ni^{3+} in the Co–Ni spine, which lowered the overpotential for $^*\text{Cl}$ formation. The small overpotentials for $^*\text{Cl}$ generation play a crucial role in enabling the efficient activation of CH_4 and subsequent conversion to CH_3Cl , thus avoiding over-oxidation to CO_2 [74]. The Cl^- -mediated environment also promoted methane oxidation to CH_3OH on Cu–Ti bimetallic oxides with 28% FE at room temperature and 72% FE at 40 °C [75].

These studies discussed above are commonly known as indirect electrochemical conversions of CH_4 to CH_3OH . The term indirect refers to strategies that use methyl sulfonate or chloromethane as an intermediate product, as well as regeneration of the reagents for methane activation. An indirect strategy that uses electrochemical methods to produce and maintain highly reactive high-valent metal species is useful. This approach can accelerate a variety of kinetically demanding reactions by accessing catalytic intermediates for the functionalization of other chemically inert substrates. However, in indirect systems, back-reaction or cross-reaction of homogeneous intermediates is a concern; therefore, careful design of cells and catalysts is required for high conversion efficiency of methane. Finally, Figure 12 schematically illustrates the advantages and disadvantages of direct and indirect methane conversion.

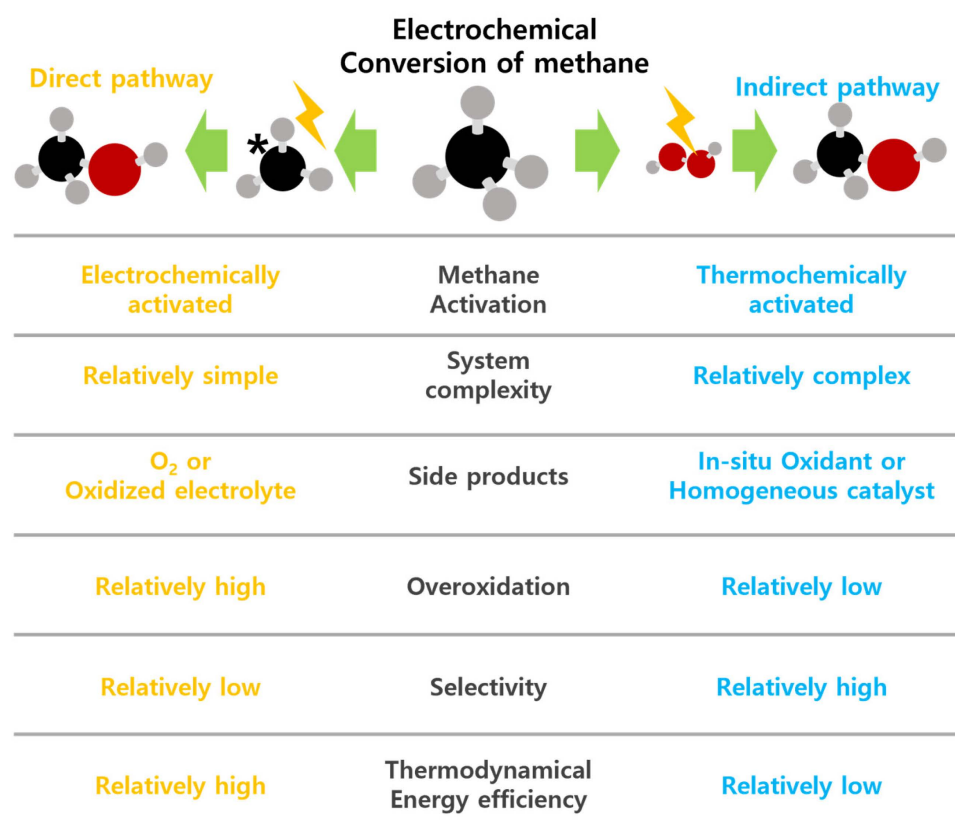


Figure 12. Schematic diagram for comparison between direct and indirect electrochemical methane oxidation.

4. Electrochemical Conversion of Methane via a MEA Structure Reactor

The MEA architecture may consist of a fully vapor-fed configuration or incorporate a liquid electrolyte solution such as carbonate or hydroxide supplied to one or both sides

of the cell. This arrangement increases the reactant concentration on the electrocatalyst by forming a gas–liquid–solid ternary-phase interface. The reactant and electrolyte are supplied through the nanostructured porous transport layer, and a high concentration of the gas reactant at the ternary-phase interface stimulates the reaction rate on the electrocatalyst. Moreover, this interface regulates the pH and microenvironment of the electrolyte within the diffusion layer. The central characteristic of the MEA architecture lies in its ability to facilitate the efficient transport of reactants and products to and from the catalyst layer while minimizing ohmic loss through the membrane. MEAs have proven to be successful in applications such as fuel cells, electrolyzers, and various energy-conversion technologies, thus making them potentially ideal architectures for the partial oxidation of methane to methanol [76,77].

As presented in Figure 13, an MEA comprises an ionically conducting separator or membrane with an anode catalyst layer on one side and a cathode catalyst layer on the opposite side. The ion-conducting medium situated between these catalyst layers can be either ceramic or polymer-based (proton- or anion-conducting), typically with a thickness of approximately 100 μm . Gas diffusion layers (GDLs) are positioned externally on catalyst layers to enhance the transport of gas-phase reactants and products. To ensure effective ion transport to and from the catalyst nanoparticles within the catalyst layers, the catalyst nanoparticles were coated with an ionomer that typically possesses properties similar to those of a membrane separator. The ionomer also acts as a bridge for ion transport through the membrane.

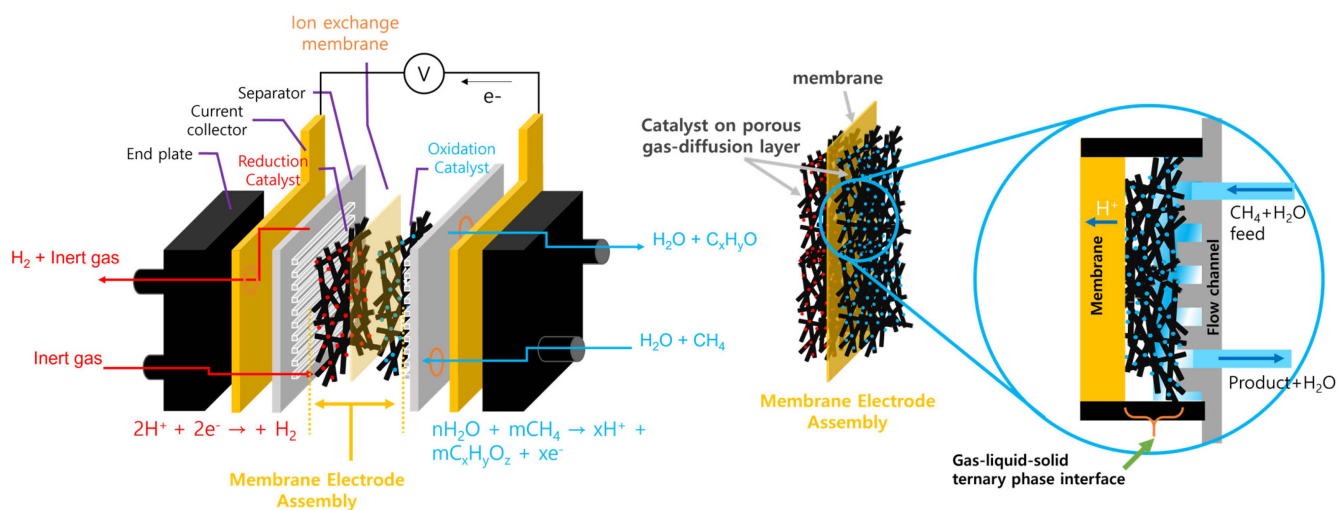


Figure 13. Schematic diagram of MEA reactor for methane oxidation.

A porous catalyst-supporting layer can function as a gas diffusion electrode (GDE) and is applicable in both aqueous and gas-fed systems [76]. The gas reactant (CH_4) can diffuse to the electrocatalyst and electrolyte through nano-sized voids in carbon-based nanoporous materials. Generally, carbon felt or carbon paper is used as a diffusion layer. Notably, controlling the cell temperature and promoting the mass transport of methanol away from the electrode surface can suppress the complete oxidation of the products. Furthermore, the transport of methanol can be improved by varying the shape of the electrode surface and optimizing the reactant gas flow [20,26,78,79]. The catalyst and ion-conducting medium (the ionomer and membrane, respectively) constitute the two pivotal components of an MEA.

The ionomer and membrane often determine the upper limit of the MEA operating temperature, and they must exhibit high ionic and electronic conductivities to minimize the internal resistance of the cell. Ceramics and polymers are membrane materials possessing distinct advantages and disadvantages. A ceramic separator demands operation within a temperature range of 100–300 $^{\circ}\text{C}$ to demonstrate effective ionic conductivities

(0.06–0.2 S/cm) [80]. Operating at elevated temperatures can enhance methane activation but may pose challenges in preventing complete oxidation [81]. A drawback of ceramic separators is their brittleness, which potentially limits their service life due to the risk of cracking. However, these separators exhibit minimum product crossover [80,82]. In contrast, polymeric membranes can achieve a conductivity of approximately 0.1 S/cm at room temperature but require full hydration for optimal performance [81,83]. Additionally, polymeric membranes often face methanol crossover issues; however, they offer the advantage of methanol recovery without further oxidation [84].

Performance-Limiting Factor of the MEA Electrochemical Reactor

The overall performance of the MEA reactor can be expressed in terms of the energy efficiency (EE), which is the product of the voltaic efficiency (VE) and Faradaic efficiency (CE), as presented in Equation (1).

$$EE = VE \times CE \quad (1)$$

Therefore, optimizing both VE and CE for efficient methane oxidation is necessary. There are various limiting factors, such as mass transportation and the number of reactions at a single electrode, and cell operating conditions, such as potential, temperature, and reactant flow rate.

First, the VE can be defined using Equation (2),

$$VE = \frac{V_{\text{thermo}}}{V_{\text{applied}}} \quad (2)$$

where V_{thermo} is the thermodynamic operating potential for methane-to-methanol conversion ($0.58 V_{\text{SHE}}$), and V_{applied} is the actual operating potential. Three primary factors limit VE. First, the transport processes in MEA are critical and must be understood to control the transportation of reactants and products. Figure 14a presents the gas and ion flows in the MEA structure during methane oxidation. The reactants, CH_4 and H_2O , should be transported to the electrocatalytic layer but not to the crossed membrane. However, protons should be transported to the cathodic electrocatalytic layer through an ion-conductive membrane, and the methanol product should not cross the membrane. However, the crossover of chemicals or poor proton transportation directly affects the VE of the MEA reactor due to the back reaction or reaction rate, which is limited by the poor mass transportation rate (mass transport losses). Second, the kinetics of the electrocatalyst are also critical for the efficiency of the overall reaction, as the overpotential of the electrocatalyst is directly related to the reaction kinetics on the catalyst surface (kinetic losses). Third, the ohmic resistance of the reactor influences the ohmic loss (VE). These three limiting factors are primarily controlled at different reaction rates (i.e., currents). For example, kinetics is the primary limiting factor for the overall reaction under low reaction rate conditions, but the ohmic resistance of the reactor becomes the primary limiting factor when the reaction rate is very high. The limiting factors controlling V_{applied} are depicted in Figure 14b, in which the ohmic losses are coupled to mass transfer as the hydration of the membrane and ionomer depends on water transport. Both of these losses can be minimized by optimizing the reaction conditions (temperature and membrane width); however, reactant or product crossover and material stability can be the result of these tradeoffs.

The CE describes the amount of current utilized for the formation of CH_3OH from CH_4 after including possible side reactions such as product crossover and reversible reduction to methane as presented in Equation (3), where

$$CE = \frac{i_{\text{methanol}} - i_{\text{crossover}}}{i_{\text{T}}} = FE - \frac{i_{\text{crossover}}}{i_{\text{T}}} \approx \frac{N_{\text{methanol}}}{\frac{i_{\text{T}}}{2F}} \quad (3)$$

i_T represents the overall current density, and i_{methanol} denotes the partial current density specifically associated with the production of methanol at the anode. In the absence of any crossover or methanol reduction to methane, CE is equivalent to the FE. The FE for methanol production can be less than 1 due to additional reactions occurring at the anode, including the OER. Generally, $i_{\text{crossover}}$ is not easily measured, and thus the CE is evaluated by quantifying the overall methanol flux (N_{methanol}) and comparing it to the corresponding total equivalent flux if all the current were transformed into methanol as determined with Faraday's law.

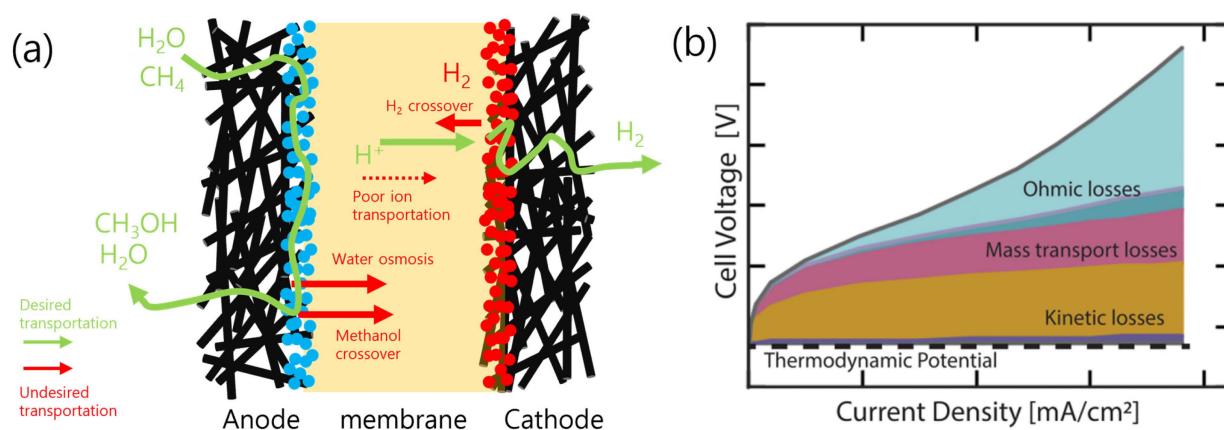


Figure 14. (a) Transportation of gas and ions through the MEA. (b) Flow of reactant, product, and other transport mechanisms. (b) Distribution of applied potential for the MEA system by current level [28]. Copyright 2020, American Chemical Society.

To accurately ascertain the total methanol flux and achieve a precise overall carbon balance, measuring the concentrations and volumetric flow rates in both the gaseous and liquid streams is necessary. Additionally, the overall volumetric flow rate exiting the cell is not equivalent to the total inlet flow rate, as different species are transported across the membrane during the reaction. Therefore, the precise determination of the outflow rate from the cell is important for the accurate quantification of the molar flow rate of the resultant products. This can be achieved using various calibrated devices and flow meters. At high current densities, precise measurement is critical, as a large amount of reactant is involved in the reaction. The use of the inlet flow, in this case, can result in inaccurate FEs [85]. Furthermore, the residence time of the gases is also important, as it can be measured from the inlet flow rate and free volume of the cell. The importance of residence time is often greater for half-cells than for MEAs, as the available volume in MEAs is mostly concentrated in the channels and backing layers. Residence time is a significant factor only in cases with high conversion rates.

The primary limiting factor for CE is the selectivity of the electrocatalyst. Generally, water oxidation is the main competitive reaction for methane oxidation under water vapor or liquid environmental conditions. Additionally, selective methanol formation without the formation of side products is important for increasing the CE of the electrocatalyst (reactor). The selectivity can also be affected by experimental conditions such as the temperature, pressure, methane solubility, or flow rate of the electrolyte. However, the most important property is the catalytic activity for the partial oxidation of methane for methanol production.

Lee et al. studied the oxidation of methane to methanol under low-temperature conditions. This investigation was conducted using a reactor designed as a fuel cell, wherein a combination of methane and water vapor was introduced to the anode while air was introduced to the cathode. Various electrocatalysts, including noble metals and transition metal oxides, were impregnated onto catalyst supports and analyzed for methanol production. Among the various catalysts, the V₂O₅/SnO₂ anode yielded noteworthy results at a temperature of 100 °C. The catalyst attains 61.4% current efficiency and 88.4% selectivity

towards methanol. Oxygen-active species are efficiently generated at the vanadium-active sites [26]. Hibino et al. investigated methanol production by mixing high-activity Pd–Au–Cu/C with proton-conducting $\text{Sn}_{0.9}\text{In}_{0.1}\text{P}_2\text{O}_7$ and reported the role of active oxygen species on the surface of the anode and cathode in a proton-exchange membrane fuel cell for the oxidation of methane to methanol at a Pd–Au/C cathode. The methanol formation (selectivity ~6.03%) was attributed to the generation of O^* as a result of an oxygen reduction reaction at the cathode surface [25]. In another study, high-activity Pd–Au–Cu/C mixed with proton-conducting $\text{Sn}_{0.9}\text{In}_{0.1}\text{P}_2\text{O}_7$ particles achieved methanol synthesis with high selectivity and yield at high temperatures and pressures. However, a mixed catalyst in a liquid system is expected to decrease the required reaction temperature and pressure [86].

MEAs follow the same reaction mechanism (radical formation) as those of conventional electrochemical systems. Santos et al. demonstrated the electrochemical partial oxidation of CH_4 using hydroxyl radicals as the oxygen source in alkaline anion exchange membrane fuel cells (AAEMFCs). The AAEMFCs achieved 20% methane conversion at room temperature over Pt/C, Pd/C, and Ni/C, with methanol and formate as primary products. Product stability and reaction pathways were identified using in situ infrared (IR) analysis. The methanol synthesis over Pt/C begins at open circuit potential (OCP) (0.3 V), and the methanol peak disappears as the potential approaches 0.0 V, thus indicating the overoxidation of CH_3OH to COO. However, the methanol band exists at all applied potentials on the Pd/C surface, although the intensity of the band decreases around 0.0 V. Ni/C also facilitates methane activation by regulating the applied potential [87]. Nandeha et al. reported the activation of CH_4 by H_2O_2 injected into the cathode of a solid membrane reactor–PEMFC at ambient temperature. The catalytic layer adsorbed both reagents on the active sites, thus resulting in the generation of $\bullet\text{OH}$ that subsequently reacted with CH_4 to produce CH_3OH [88]. However, in a carbonate electrolyte system, negatively charged oxygen in CO_3^{2-} was the primary source of oxygen. In addition to methanol, carbonate-exchange MEAs yielded various additional products, such as $\text{C}_2\text{H}_5\text{OH}$, $\text{C}_3\text{H}_7\text{OH}$, HCHO, CO, HCOOH, and ethers. These exchange MEAs were employed to evaluate the catalytic activity of Ni, Co, and Fe catalysts that exhibit instability under acidic conditions [33–35].

Rocha et al. designed $\text{TiO}_2/\text{RuO}_2/\text{PTFE}$ GDEs for methane conversion to methanol in a 0.1 M Na_2SO_4 solution. This system achieved ~30% current efficiency for methanol formation at 2.2 V_{SCE} , along with the formation of 10% formaldehyde, 40% formic acid, and 20% O_2 . In a follow-up study, Rocha et al. incorporated V_2O_5 into $\text{TiO}_2/\text{RuO}_2/\text{PTFE}$ to enhance methanol selectivity. The methanol formation rate increased twice at 2.0 V_{SCE} when 5.6% V_2O_5 was added to $\text{TiO}_2/\text{RuO}_2$ by assuming the formation of formaldehyde and formic acid [63,89]. Reported studies on electrochemical methane oxidation have used both aqueous electrolyte cells and MEAs. In all published studies on methane oxidation (Table 3), the selection criteria for the electrocatalysts are not well reported. Most of the materials selected for methane oxidation are also highly active on OERs; however, no detailed explanation is given as to why these materials are expected to be active in methane oxidation. Table 3 summarizes the reported studies focused on low-temperature electrochemical methane oxidation in both MEAs and half-cells.

Table 3. Experimental results for low-temperature electrochemical methane conversion via MEA reactors.

Electrode	Temperature (°C)	Potential (V)	Electrolyte/Membrane	Oxidant	Product (Production Rate)	Current Density (mA/cm ²)	Ref.
$\text{V}_2\text{O}_5/\text{SnO}_2\text{-PTFE}$ anode	100	0.9	$\text{Sn}_{0.9}\text{In}_{0.1}\text{P}_2\text{O}_7$	H_2O	CH_3OH	4	[26]
PdAu/C cathode	50		$\text{Sn}_{0.9}\text{In}_{0.1}\text{P}_2\text{O}_7$	O_2	CH_3OH ($0.4 \mu\text{mol h}^{-1} \text{cm}^{-2}$),	400	[25]
Pt/C cathode	85	0.4	Nafion 117	H_2O_2	CH_3OH (0.14 mol L^{-1})		[88]

Table 3. Cont.

Electrode	Temperature (°C)	Potential (V)	Electrolyte/Membrane	Oxidant	Product (Production Rate)	Current Density (mA/cm ²)	Ref.
NiO-ZrO ₂ anode	40	2.0	1.0 M Na ₂ CO ₃ + DMF/ralex AM-PAD	CO ₃ ²⁻	CH ₃ OH, HCHO, CO, HCOOH, C ₂ H ₅ OH, CH ₃ COOH, CH ₃ COCH ₃ , CH ₃ CHOHCH ₃	21	[33]
Co ₃ O ₄ -ZrO ₂ /CP-nafion 117 anode	25	2.0 V _{Pt}	0.5 M Na ₂ CO ₃ /Nafion 117	CO ₃ ²⁻	CH ₃ OH (9.9 μg L ⁻¹ h ⁻¹), CH ₂ O, C ₂ H ₅ OH, C ₂ H ₄ O, C ₃ H ₈ O, C ₃ H ₆ O	~10	[34, 35]
Pd/C Anode	80	0.05–1.2 V	Nafion	H ₂ O	HCOOH	~10	[90]
PdZn/C Anode	80	0.05–1.2 V	Nafion	H ₂ O	CH ₃ OH, HCOOH	~10	[91]
PdAu/C Anode	80	0.05–1.2 V	Nafion	H ₂ O	CH ₃ OH, HCOOH	~10	[92]
Pd/C, Pt/C, Ni/C anode	25 (anode) 85 (cathode)	0.3	6.0 M KOH/Nafion 117	OH ⁻	CH ₃ OH (0.9 mol L ⁻¹)	~1	[87]
MO _x anode (M = Mn, Fe, Ni, Os, Pt)	160	--	KOH + H ₂ O (catholyte)/ion exchange membrane	OH ⁻	CH ₃ OH	--	[93]
MO _x anode (M = Ni, Co, Cu, Ag, Pt, Au, Ce, Pb, Fe, Mn, Zn Os, Pt)	25–160	--	KOH + H ₂ O (catholyte)/Daramic anion exchange membrane	OH ⁻	CH ₃ OH, CO ₂	--	[94]
[6,6'-(2,2'-Bipyridine-6,6'-Diyl)bis(1,3,5-Triazine-2,4-Diamine)](Nitrate-O)Copper(II) Complex/C Anode	25	0.2–0.3	KOH-doped Nafion membrane	OH ⁻	CH ₃ OH (1.85 mol L ⁻¹ h ⁻¹), HCOOH	~1	[95]
TiO ₂ /RuO ₂ /V ₂ O ₅ /anode	25	2.0 V _{SCE}	0.1 M Na ₂ SO ₄ /PTFE	H ₂ O (OH ⁻)	CH ₃ OH (300 mg L ⁻¹ h ⁻¹), HCHO	57	[63]
TiO ₂ /RuO ₂ anode	25	2.1 V _{SCE}	0.1 M Na ₂ SO ₄ /PTFE	H ₂ O (OH ⁻)	CH ₃ OH (220 mg L ⁻¹ cm ²), HCHO, HCOOH	30	[89]

5. Conclusions and Outlook

In this review, we summarize the developments in electrochemical CH₄ conversion under ambient conditions. We discuss electrochemical strategies for the activation of C-H bonds and the stability control of intermediates. Despite significant efforts to enhance CH₄ conversion and selectivity, considerable challenges persist for practical CH₄ utilization. This review highlights the complexities of low-temperature CH₄ electroconversion while focusing on the electrolyte role and yield optimization for methanol and higher alcohols. Significant challenges in low-temperature electroconversion of CH₄ require innovative solutions and collaborative efforts across various scientific domains. Despite promising strategies employing high-valence metal catalysts, issues such as competitive reactions and electrolyte stability persist. Overcoming these challenges necessitates the exploration of alternative redox pairs compatible with water and the development of catalysts that protect the products from overoxidation, thus making them viable for industrial applications. Additionally, the utilization of indirect electrochemical methods that require the in situ generation of oxidizing agents holds potential but requires further investigation to avoid extreme conditions and high economic value.

Direct electrochemical conversion requires a shift from theoretical understanding to practical implementation. Innovative catalyst designs, including MXenes, bimetallic materials, metal oxides with low Madelung potentials, and high-entropy oxides supported by porous structures, can significantly enhance CH₄ oxidation to alcohols. Doping and interface engineering can be further sought [96]. The direct conversion process involves the

generation of reactive oxygen species (ROS) at the catalyst surface, which then interacts with methane to produce oxygenated products. However, significant challenges associated with this approach include the solubility of methane in solution, the effect of adsorption–desorption kinetics on overoxidation, and the high overpotentials required to drive the reaction forward. This often involves competition between the OER and methane oxidation that can be circumvented by the use of oxidants other than water, such as CO_3^{2-} and OH^- . The adsorption and desorption activities of methane can be optimized by employing highly active surface areas and intrinsic catalytic activities such as nickel-based electrocatalysts and metal–organic frameworks (MOF). The development of nickel composite catalysts with MOFs may represent a good strategy for enhancing catalytic efficiency. In comparison, indirect methane conversion has exhibited interesting preliminary results; however, this approach requires expensive noble metals as oxidizing agents and harsh reaction conditions. The electrochemical in situ generation of oxidizing agents such as H_2O_2 may be a promising strategy for the generation of value-added products.

Addressing issues related to electrolyte engineering and product separation is pivotal for minimizing overoxidation and improving selectivity, ultimately bringing us closer to achieving the goal of commercialization. Systematic studies are required to address the variability in the experimental conditions. Understanding the importance of factors such as potential, current, temperature, and CH_4 pressure is critical for enhancing product yield. Additionally, advanced analytical techniques and real-time spectroscopy will be helpful for revealing the catalyst states and intermediate species, ultimately facilitating the design of novel catalysts. Furthermore, innovations in reactor design and detailed techno-economic analyses are important for scaling up electrochemical systems to meet industrial demands.

A comprehensive techno-economic analysis provides the economic viability of a methane-to-methanol fuel cell system that exhibits methanol selectivity of 70% at a cell potential of approximately 0.5 V, providing 100 mA cm^{-2} within the temperature range of 100 to 250 °C [29]. Existing electrocatalysts exhibit inadequacy with regard to meeting actual demands. The primary challenge in achieving this goal is the development of an efficient electrocatalyst that can selectively convert methane to value-added products at low potential and high currents under mild reaction conditions.

In addition, electrochemical methane oxidation can be coupled with other opposite cathodic reactions. In an aqueous electrolyte, when methane is oxidized at the anode, hydrogen is produced at the cathode. However, by changing the material at the cathode while the methane is oxidized, other value-added products can be synthesized at the cathode. For example, if the cathode for electrochemical CO_2 reduction is used, alcohol at both the anode and cathode can be produced simultaneously [97–99]. However, this kind of co-production of alcohol (or co-production of other value-added chemicals) can only be performed in a certain voltage range due to competing reactions such as the oxygen evolution reaction or the hydrogen evolution reaction at each electrode. Therefore, it is important to determine the appropriate operating potential for co-production of the target product. The operating potential can be estimated from the electrocatalytic activity of each half-cell.

Enhancing the efficiency and selectivity of CH_4 conversion using electrochemical methods is challenging. However, efficiency and selectivity can be increased by enhancing methane solubility. The solubility of methane can be enhanced by employing a solid–liquid–gas ternary phase at the interface of the electrocatalyst/gas diffusion layer in the electrolyte that allows CH_4 gas to be introduced into the active sites of the electrolyte through a gas diffusion layer. Additionally, the exploration of appropriate organic solvents is a promising approach to overcome the low solubility of CH_4 in water. Organic solvents may yield products that are different from those obtained using aqueous electrolytes. However, these solvents are less susceptible to electrocatalytic oxidation than water. The development of novel electrocatalysts for CH_4 production to produce valuable $\text{C}_{2/2+}$ products is an important research topic. Overcoming the challenges related to low electrical conductivity and high charge transfer resistance at the interface by designing carbon-based composites

and doping foreign elements into the active electrocatalysts will improve the catalytic activity by altering the electronic properties.

Understanding the rate-determining step (RDS) is important for the development of efficient electrocatalysts. Investigating the charge-transfer mechanism using in situ and operando spectroscopy, along with in situ characterizations such as X-ray diffraction (XRD), transmission electron microscopy (TEM), and IR spectroscopy coupled with DFT calculations, can provide valuable insights for modifying existing electrocatalysts and designing new ones [100]. Moreover, techno-economic analyses incorporating device fabrication costs and methanol purification processes are pivotal for setting performance benchmarks.

Author Contributions: Conceptualization, E.D.P.; writing—original draft preparation, A.M.; writing—review and editing, E.D.P. and S.Y.C.; supervision, project administration, and funding acquisition, E.D.P. All authors have read and agreed to the published version of the manuscript.

Funding: This study was supported by the C1 Gas Refinery Program through the National Research Foundation of Korea (NRF) and funded by the Ministry of Science, ICT, and Future Planning (2015M3D3A1A01064899).

Data Availability Statement: Not applicable.

Conflicts of Interest: The authors declare no conflicts of interest.

References

1. Meng, X.; Cui, X.; Rajan, N.P.; Yu, L.; Deng, D.; Bao, X. Direct Methane Conversion under Mild Condition by Thermo-, Electro-, or Photocatalysis. *Chem* **2019**, *5*, 2296–2325. [\[CrossRef\]](#)
2. Richard, D.; Huang, Y.-C.; Morales-Guio, C.G. Recent advances in the electrochemical production of chemicals from methane. *Curr. Opin. Electrochem.* **2021**, *30*, 100793. [\[CrossRef\]](#)
3. Soucie, H.; Elam, M.; Mustain, W.E. Practical Assessment for At-Scale Electrochemical Conversion of Methane to Methanol. *ACS Energy Lett.* **2023**, *8*, 1218–1229. [\[CrossRef\]](#)
4. Zakaria, Z.; Kamarudin, S.K. Direct conversion technologies of methane to methanol: An overview. *Renew. Sustain. Energy Rev.* **2016**, *65*, 250–261. [\[CrossRef\]](#)
5. Huang, K.; Miller, J.B.; Huber, G.W.; Dumesic, J.A.; Maravelias, C.T. A General Framework for the Evaluation of Direct Nonoxidative Methane Conversion Strategies. *Joule* **2018**, *2*, 349–365. [\[CrossRef\]](#)
6. Jackson, R.B.; Saunio, M.; Bousquet, P.; Canadell, J.G.; Poulter, B.; Stavert, A.R.; Bergamaschi, P.; Niwa, Y.; Segers, A.; Tsuruta, A. Increasing anthropogenic methane emissions arise equally from agricultural and fossil fuel sources. *Environ. Res. Lett.* **2020**, *15*, 071002. [\[CrossRef\]](#)
7. Hussin, F.; Aroua, M.K. Recent development in the electrochemical conversion of carbon dioxide: Short review. *AIP Conf. Proc.* **2019**, *2124*, 030017. [\[CrossRef\]](#)
8. Arminio-Ravelo, J.A.; Escudero-Escribano, M. Strategies toward the sustainable electrochemical oxidation of methane to methanol. *Curr. Opin. Green Sustain. Chem.* **2021**, *30*, 100489. [\[CrossRef\]](#)
9. Abdelkader Mohamed, A.G.; Zahra Naqviab, S.A.; Wang, Y. Advances and Fundamental Understanding of Electrocatalytic Methane Oxidation. *ChemCatChem* **2021**, *13*, 787–805. [\[CrossRef\]](#)
10. Wang, Q.; Kan, M.; Han, Q.; Zheng, G. Electrochemical Methane Conversion. *Small Struct.* **2021**, *2*, 2100037. [\[CrossRef\]](#)
11. Bagherzadeh Mostaghimi, A.H.; Al-Attas, T.A.; Kibria, M.G.; Siahrostami, S. A review on electrocatalytic oxidation of methane to oxygenates. *J. Mater. Chem. A* **2020**, *8*, 15575–15590. [\[CrossRef\]](#)
12. Dhandole, L.K.; Kim, S.H.; Moon, G.-h. Understanding (photo)electrocatalysis for the conversion of methane to valuable chemicals through partial oxidation processes. *J. Mater. Chem. A* **2022**, *10*, 19107–19128. [\[CrossRef\]](#)
13. Jang, J.; Shen, K.; Morales-Guio, C.G. Electrochemical Direct Partial Oxidation of Methane to Methanol. *Joule* **2019**, *3*, 2589–2593. [\[CrossRef\]](#)
14. Shi, T.; Sridhar, D.; Zeng, L.; Chen, A. Recent advances in catalyst design for the electrochemical and photoelectrochemical conversion of methane to value-added products. *Electrochem. Commun.* **2022**, *135*, 107220. [\[CrossRef\]](#)
15. Upham, D.C.; Kristoffersen, H.H.; Snodgrass, Z.R.; Gordon, M.J.; Metiu, H.; McFarland, E.W. Bromine and iodine for selective partial oxidation of propane and methane. *Appl. Catal. A* **2019**, *580*, 102–110. [\[CrossRef\]](#)
16. Schwach, P.; Pan, X.; Bao, X. Direct Conversion of Methane to Value-Added Chemicals over Heterogeneous Catalysts: Challenges and Prospects. *Chem. Rev.* **2017**, *117*, 8497–8520. [\[CrossRef\]](#)
17. Liu, Z.; Xu, B.; Jiang, Y.-J.; Zhou, Y.; Sun, X.; Wang, Y.; Zhu, W. Photocatalytic Conversion of Methane: Current State of the Art, Challenges, and Future Perspectives. *ACS Environ. Au* **2023**, *3*, 252–276. [\[CrossRef\]](#)
18. Xie, S.; Lin, S.; Zhang, Q.; Tian, Z.; Wang, Y. Selective electrocatalytic conversion of methane to fuels and chemicals. *J. Energy Chem.* **2018**, *27*, 1629–1636. [\[CrossRef\]](#)

19. Seh, Z.W.; Kibsgaard, J.; Dickens, C.F.; Chorkendorff, I.; Nørskov, J.K.; Jaramillo, T.F. Combining theory and experiment in electrocatalysis: Insights into materials design. *Science* **2017**, *355*, eaad4998. [[CrossRef](#)]
20. Arnarson, L.; Schmidt, P.S.; Pandey, M.; Bagger, A.; Thygesen, K.S.; Stephens, I.E.L.; Rossmeisl, J. Fundamental limitation of electrocatalytic methane conversion to methanol. *Phys. Chem. Chem. Phys.* **2018**, *20*, 11152–11159. [[CrossRef](#)]
21. Sher Shah, M.S.A.; Oh, C.; Park, H.; Hwang, Y.J.; Ma, M.; Park, J.H. Catalytic Oxidation of Methane to Oxygenated Products: Recent Advancements and Prospects for Electrocatalytic and Photocatalytic Conversion at Low Temperatures. *Adv. Sci.* **2020**, *7*, 2001946. [[CrossRef](#)]
22. O'Reilly, M.E.; Kim, R.S.; Oh, S.; Surendranath, Y. Catalytic Methane Monofunctionalization by an Electrogenerated High-Valent Pd Intermediate. *ACS Cent. Sci.* **2017**, *3*, 1174–1179. [[CrossRef](#)] [[PubMed](#)]
23. Stoukides, M.; Eng, D.; Chiang, P.H.; Alqahtany, H. Electrochemical Modification of the Activity and Selectivity of Metal Catalysts. In *Studies in Surface Science and Catalysis*; Gucci, L., Solymosi, F., TÉTÉNYI, P., Eds.; Elsevier: Amsterdam, The Netherlands, 1993; Volume 75, pp. 2131–2134.
24. Patterson, B.D.; Mo, F.; Borgschulte, A.; Hillestad, M.; Joos, F.; Kristiansen, T.; Sunde, S.; van Bokhoven, J.A. Renewable CO₂ recycling and synthetic fuel production in a marine environment. *Proc. Natl. Acad. Sci. USA* **2019**, *116*, 12212–12219. [[CrossRef](#)] [[PubMed](#)]
25. Tomita, A.; Nakajima, J.; Hibino, T. Direct Oxidation of Methane to Methanol at Low Temperature and Pressure in an Electrochemical Fuel Cell. *Angew. Chem. Int. Ed.* **2008**, *47*, 1462–1464. [[CrossRef](#)]
26. Lee, B.; Hibino, T. Efficient and selective formation of methanol from methane in a fuel cell-type reactor. *J. Catal.* **2011**, *279*, 233–240. [[CrossRef](#)]
27. Sobyenin, V.A.; Belyaev, V.D. Gas-phase electrocatalysis: Methane oxidation to syngas in a solid oxide fuel cell reactor. *Solid State Ionics* **2000**, *136–137*, 747–752. [[CrossRef](#)]
28. Fornaciari, J.C.; Primc, D.; Kawashima, K.; Wygant, B.R.; Verma, S.; Spanu, L.; Mullins, C.B.; Bell, A.T.; Weber, A.Z. A Perspective on the Electrochemical Oxidation of Methane to Methanol in Membrane Electrode Assemblies. *ACS Energy Lett.* **2020**, *5*, 2954–2963. [[CrossRef](#)]
29. Promopattam, P.; Viswanathan, V. Identifying Material and Device Targets for a Flare Gas Recovery System Utilizing Electrochemical Conversion of Methane to Methanol. *ACS Sustain. Chem. Eng.* **2016**, *4*, 1736–1745. [[CrossRef](#)]
30. Jiang, H.; Zhang, L.; Han, Z.; Tang, Y.; Sun, Y.; Wan, P.; Chen, Y.; Argyle, M.D.; Fan, M. Direct conversion of methane to methanol by electrochemical methods. *Green Energy Environ.* **2022**, *7*, 1132–1142. [[CrossRef](#)]
31. Kishore, M.R.A.; Lee, S.; Yoo, J.S. Fundamental Limitation in Electrochemical Methane Oxidation to Alcohol: A Review and Theoretical Perspective on Overcoming It. *Adv. Sci.* **2023**, *10*, 2301912. [[CrossRef](#)]
32. Amenomiya, Y.; Birrs, V.I.; Goledzinowski, M.; Galuszka, J.; Sanger, A.R. Conversion of Methane by Oxidative Coupling. *Catal. Rev.-Sci. Eng.* **1990**, *32*, 163–227. [[CrossRef](#)]
33. Spinner, N.; Mustain, W.E. Electrochemical Methane Activation and Conversion to Oxygenates at Room Temperature. *J. Electrochem. Soc.* **2013**, *53*, 1. [[CrossRef](#)]
34. Ma, M.; Jin, B.J.; Li, P.; Jung, M.S.; Kim, J.I.; Cho, Y.; Kim, S.; Moon, J.H.; Park, J.H. Ultrahigh Electrocatalytic Conversion of Methane at Room Temperature. *Adv. Sci.* **2017**, *4*, 1700379. [[CrossRef](#)] [[PubMed](#)]
35. Ma, M.; Oh, C.; Kim, J.; Moon, J.H.; Park, J.H. Electrochemical CH₄ oxidation into acids and ketones on ZrO₂:NiCo₂O₄ quasi-solid solution nanowire catalyst. *Appl. Catal. B* **2019**, *259*, 118095. [[CrossRef](#)]
36. Kaur, M.; Li, Z.; Meng, S.; Li, W.; Song, H. Electrocatalytic methane conversion to high value chemicals at ambient conditions. *Energy Convers. Manag.* **2023**, *285*, 117029. [[CrossRef](#)]
37. Oh, C.; Kim, J.; Hwang, Y.J.; Ma, M.; Park, J.H. Electrocatalytic methane oxidation on Co₃O₄-incorporated ZrO₂ nanotube powder. *Appl. Catal. B* **2021**, *283*, 119653. [[CrossRef](#)]
38. Qiao, J.; Li, H.F.; Chang, Y.; Guan, L.S.; Shuang, S.; Dong, C. Voltammetric Study and Detection of Methane on Nickel Hydroxide-Modified Nickel Electrode. *Anal. Lett.* **2008**, *41*, 593–598. [[CrossRef](#)]
39. Omasta, T.J.; Rigdon, W.A.; Lewis, C.A.; Stanis, R.J.; Liu, R.; Fan, C.Q.; Mustain, W.E. Two Pathways for Near Room Temperature Electrochemical Conversion of Methane to Methanol. *ECS Trans.* **2015**, *66*, 129. [[CrossRef](#)]
40. Kadosh, Y.; Ben-Eliyahu, Y.; Bochlín, Y.; Ezuz, L.; Iflah, Y.; Halevy, S.; Kozuch, S.; Korin, E.; Bettelheim, A. A bilayer coating as an oxygen-transfer cascade for the electrochemical ambient conversion of methane to oxygenates. *Chem. Commun.* **2022**, *58*, 3154–3157. [[CrossRef](#)]
41. Xu, N.; Coco, C.A.; Wang, Y.; Su, T.; Wang, Y.; Peng, L.; Zhang, Y.; Liu, Y.; Qiao, J.; Zhou, X.-D. Electro-conversion of methane to alcohols on “capsule-like” binary metal oxide catalysts. *Appl. Catal. B* **2021**, *282*, 119572. [[CrossRef](#)]
42. Luo, M.; Li, J.; Wang, M.; Ma, Y.; Zheng, G.; Wang, M.; Zhou, Y. Electrooxidation of methane to acetic acid over ZnO nanosheets: Defect-sites engineering. *J. Environ. Chem. Eng.* **2023**, *11*, 109539. [[CrossRef](#)]
43. Ponticorvo, E.; Iuliano, M.; Cirillo, C.; Sarno, M. Selective C₂ electrochemical synthesis from methane on modified alumina supporting single atom catalysts. *Chem. Eng. J.* **2023**, *451*, 139074. [[CrossRef](#)]
44. Kim, C.; Min, H.; Kim, J.; Sul, J.; Yang, J.; Moon, J.H. NiO/ZnO heterojunction nanorod catalyst for high-efficiency electrochemical conversion of methane. *Appl. Catal. B* **2023**, *323*, 122129. [[CrossRef](#)]

45. Song, Y.; Zhao, Y.; Nan, G.; Chen, W.; Guo, Z.; Li, S.; Tang, Z.; Wei, W.; Sun, Y. Electrocatalytic oxidation of methane to ethanol via NiO/Ni interface. *Appl. Catal. B* **2020**, *270*, 118888. [[CrossRef](#)]
46. Guo, Z.; Chen, W.; Song, Y.; Dong, X.; Li, G.; Wei, W.; Sun, Y. Efficient methane electrocatalytic conversion over a Ni-based hollow fiber electrode. *Chin. J. Catal.* **2020**, *41*, 1067–1072. [[CrossRef](#)]
47. Xie, Z.; Chen, M.; Chen, Y.; Guan, A.; Han, Q.; Zheng, G. Electrocatalytic Methane Oxidation to Ethanol via Rh/ZnO Nanosheets. *J. Phys. Chem. C* **2021**, *125*, 13324–13330. [[CrossRef](#)]
48. Kim, C.; Min, H.; Kim, J.; Moon, J.H. Boosting electrochemical methane conversion by oxygen evolution reactions on Fe–N–C single atom catalysts. *Energy Environ. Sci.* **2023**, *16*, 3158–3165. [[CrossRef](#)]
49. Ramos, A.S.; Santos, M.C.L.; Godoi, C.M.; Oliveira Neto, A.; Fernando Brambilla De Souza, R. Obtaining C₂ and C₃ Products from Methane Using Pd/C as Anode in a Solid Fuel Cell-type Electrolyte Reactor. *ChemCatChem* **2020**, *12*, 4517–4521. [[CrossRef](#)]
50. Hibino, T.; Kobayashi, K.; Nagao, M.; Zhou, D.; Chen, S.; Yamamoto, Y. Alternating Current Electrolysis for Individual Synthesis of Methanol and Ethane from Methane in a Thermo-electrochemical Cell. *ACS Catal.* **2023**, *13*, 8890–8901. [[CrossRef](#)]
51. Li, J.; Luo, M.; Wang, M.; Ma, Y.; Zheng, G.; Wang, M.; Zhou, Y.; Lu, Y.; Zhu, C.; Chen, B. Electrocatalytic conversion of methane to ethanol by ultrathin WO₃ nanosheets: Oxygen vacancy engineering. *Appl. Mater. Today* **2023**, *32*, 101855. [[CrossRef](#)]
52. Santos, M.C.L.; Godoi, C.M.; Kang, H.S.; de Souza, R.F.B.; Ramos, A.S.; Antolini, E.; Neto, A.O. Effect of Ni content in PdNi/C anode catalysts on power and methanol co-generation in alkaline direct methane fuel cell type. *J. Colloid Interface Sci.* **2020**, *578*, 390–401. [[CrossRef](#)] [[PubMed](#)]
53. Sarno, M.; Ponticorvo, E.; Funicello, N.; De Pasquale, S. Methane electrochemical oxidation at low temperature on Rh single atom/NiO/V₂O₅ nanocomposite. *Appl. Catal. A* **2020**, *603*, 117746. [[CrossRef](#)]
54. Godoi, C.M.; Santos, M.C.L.; Silva, A.J.; Tagomori, T.L.; Ramos, A.S.; de Souza, R.F.B.; Neto, A.O. Methane conversion to higher value-added product and energy co-generation using anodes OF PdCu/C in a solid electrolyte reactor: Alkaline fuel cell type monitored by differential mass spectroscopy. *Res. Chem. Intermed.* **2021**, *47*, 743–757. [[CrossRef](#)]
55. Hsieh, C.-T.; Tang, Y.-T.; Ho, Y.-S.; Shao, W.-K.; Cheng, M.-J. Methane to Methanol Conversion over N-Doped Graphene Facilitated by Electrochemical Oxygen Evolution: A First-Principles Study. *J. Phys. Chem. C* **2023**, *127*, 308–318. [[CrossRef](#)]
56. Kang, Y.; Li, Z.; Lv, X.; Song, W.; Wei, Y.; Zhang, X.; Liu, J.; Zhao, Z. Active oxygen promoted electrochemical conversion of methane on two-dimensional carbide (MXenes): From stability, reactivity and selectivity. *J. Catal.* **2021**, *393*, 20–29. [[CrossRef](#)]
57. Prajapati, A.; Collins, B.A.; Goodpaster, J.D.; Singh, M.R. Fundamental insight into electrochemical oxidation of methane towards methanol on transition metal oxides. *Proc. Natl. Acad. Sci. USA* **2021**, *118*, e2023233118. [[CrossRef](#)] [[PubMed](#)]
58. Su, Z.-Y.; Jiang, H.-M.; Han, Z.-W.; Zhang, L.-T.; Tang, Y.; Wan, P.-Y.; Khan, Z.U.H.; Chen, Y.-M. Direct Conversion of Methane to Methanol on LaCo_{0.5}Fe_{0.5}O₃ Anode in Aqueous Ionic Liquid. *Int. J. Electrochem. Sci.* **2022**, *17*, 221161. [[CrossRef](#)]
59. Zeng, L.; Thiruppathi, A.R.; van der Zalm, J.; Shi, T.; Chen, A. Tailoring trimetallic CoNiFe oxide nanostructured catalysts for the efficient electrochemical conversion of methane to methanol. *J. Mater. Chem. A* **2022**, *10*, 15012–15025. [[CrossRef](#)]
60. Shen, K.; Kumari, S.; Huang, Y.-C.; Jang, J.; Sautet, P.; Morales-Guio, C.G. Electrochemical Oxidation of Methane to Methanol on Electrodeposited Transition Metal Oxides. *J. Am. Chem. Soc.* **2023**, *145*, 6927–6943. [[CrossRef](#)]
61. Lee, J.; Yang, J.; Moon, J.H. Solar Cell-Powered Electrochemical Methane-to-Methanol Conversion with CuO/CeO₂ Catalysts. *ACS Energy Lett.* **2021**, *6*, 893–899. [[CrossRef](#)]
62. Kim, R.S.; Surendranath, Y. Electrochemical Reoxidation Enables Continuous Methane-to-Methanol Catalysis with Aqueous Pt Salts. *ACS Cent. Sci.* **2019**, *5*, 1179–1186. [[CrossRef](#)] [[PubMed](#)]
63. Rocha, R.S.; Reis, R.M.; Lanza, M.R.V.; Bertazzoli, R. Electrosynthesis of methanol from methane: The role of V₂O₅ in the reaction selectivity for methanol of a TiO₂/RuO₂/V₂O₅ gas diffusion electrode. *Electrochim. Acta* **2013**, *87*, 606–610. [[CrossRef](#)]
64. Cook, R.L.; Sammells, A.F. Ambient Temperature Methane Activation to Condensed Species under Cathodic Conditions. *J. Electrochem. Soc.* **1990**, *137*, 2007. [[CrossRef](#)]
65. Latimer, A.A.; Kakekhani, A.; Kulkarni, A.R.; Nørskov, J.K. Direct Methane to Methanol: The Selectivity–Conversion Limit and Design Strategies. *ACS Catal.* **2018**, *8*, 6894–6907. [[CrossRef](#)]
66. Ogura, K.; Migita, C.T.; Ito, Y. Combined Photochemical and Electrochemical Oxidation of Methane. *J. Electrochem. Soc.* **1990**, *137*, 500. [[CrossRef](#)]
67. Frese, K.W., Jr. Partial electrochemical oxidation of methane under mild conditions. *Langmuir* **1991**, *7*, 13–15. [[CrossRef](#)]
68. Gunsalus, N.J.; Koppaka, A.; Park, S.H.; Bischof, S.M.; Hashiguchi, B.G.; Periana, R.A. Homogeneous Functionalization of Methane. *Chem. Rev.* **2017**, *117*, 8521–8573. [[CrossRef](#)]
69. Deng, J.; Lin, S.-C.; Fuller, J.; Iñiguez, J.A.; Xiang, D.; Yang, D.; Chan, G.; Chen, H.M.; Alexandrova, A.N.; Liu, C. Ambient methane functionalization initiated by electrochemical oxidation of a vanadium (V)-oxo dimer. *Nat. Commun.* **2020**, *11*, 3686. [[CrossRef](#)]
70. Kim, R.S.; Nazemi, A.; Cundari, T.R.; Surendranath, Y. A PdIII Sulfate Dimer Initiates Rapid Methane Monofunctionalization by H Atom Abstraction. *ACS Catal.* **2020**, *10*, 14782–14792. [[CrossRef](#)]
71. Natinsky, B.S.; Lu, S.; Copeland, E.D.; Quintana, J.C.; Liu, C. Solution Catalytic Cycle of Incompatible Steps for Ambient Air Oxidation of Methane to Methanol. *ACS Cent. Sci.* **2019**, *5*, 1584–1590. [[CrossRef](#)]
72. Dang, H.T.; Lee, H.W.; Lee, J.; Choo, H.; Hong, S.H.; Cheong, M.; Lee, H. Enhanced Catalytic Activity of (DMSO)₂PtCl₂ for the Methane Oxidation in the SO₃–H₂SO₄ System. *ACS Catal.* **2018**, *8*, 11854–11862. [[CrossRef](#)]

73. Zimmermann, T.; Soorholtz, M.; Bilke, M.; Schüth, F. Selective Methane Oxidation Catalyzed by Platinum Salts in Oleum at Turnover Frequencies of Large-Scale Industrial Processes. *J. Am. Chem. Soc.* **2016**, *138*, 12395–12400. [[CrossRef](#)] [[PubMed](#)]
74. Wang, Q.; Li, T.; Yang, C.; Chen, M.; Guan, A.; Yang, L.; Li, S.; Lv, X.; Wang, Y.; Zheng, G. Electrocatalytic Methane Oxidation Greatly Promoted by Chlorine Intermediates. *Angew. Chem. Int. Ed.* **2021**, *60*, 17398–17403. [[CrossRef](#)] [[PubMed](#)]
75. Prajapati, A.; Sartape, R.; Kani, N.C.; Gauthier, J.A.; Singh, M.R. Chloride-Promoted High-Rate Ambient Electrooxidation of Methane to Methanol on Patterned Cu–Ti Bimetallic Oxides. *ACS Catal.* **2022**, *12*, 14321–14329. [[CrossRef](#)]
76. Higgins, D.; Hahn, C.; Xiang, C.; Jaramillo, T.F.; Weber, A.Z. Gas-Diffusion Electrodes for Carbon Dioxide Reduction: A New Paradigm. *ACS Energy Lett.* **2019**, *4*, 317–324. [[CrossRef](#)]
77. Weng, L.-C.; Bell, A.T.; Weber, A.Z. Towards membrane-electrode assembly systems for CO₂ reduction: A modeling study. *Energy Environ. Sci.* **2019**, *12*, 1950–1968. [[CrossRef](#)]
78. Seidel, Y.E.; Schneider, A.; Jusys, Z.; Wickman, B.; Kasemo, B.; Behm, R.J. Transport Effects in the Electrooxidation of Methanol Studied on Nanostructured Pt/Glassy Carbon Electrodes. *Langmuir* **2010**, *26*, 3569–3578. [[CrossRef](#)]
79. Márquez-Montes, R.A.; Collins-Martínez, V.H.; Pérez-Reyes, I.; Chávez-Flores, D.; Graeve, O.A.; Ramos-Sánchez, V.H. Electrochemical Engineering Assessment of a Novel 3D-Printed Filter-Press Electrochemical Reactor for Multipurpose Laboratory Applications. *ACS Sustain. Chem. Eng.* **2020**, *8*, 3896–3905. [[CrossRef](#)]
80. Heo, P.; Kajiyama, N.; Kobayashi, K.; Nagao, M.; Sano, M.; Hibino, T. Proton Conduction in Sn_{0.95}Al_{0.05}P₂O₇–PBI–PTFE Composite Membrane. *Electrochem. Solid-State Lett.* **2008**, *11*, B91. [[CrossRef](#)]
81. Heo, P.; Ito, K.; Tomita, A.; Hibino, T. A Proton-Conducting Fuel Cell Operating with Hydrocarbon Fuels. *Angew. Chem. Int. Ed.* **2008**, *47*, 7841–7844. [[CrossRef](#)]
82. Paschos, O.; Kunze, J.; Stimming, U.; Maglia, F. A review on phosphate based, solid state, protonic conductors for intermediate temperature fuel cells. *J. Phys. Condens. Matter* **2011**, *23*, 234110. [[CrossRef](#)]
83. Kusoglu, A.; Weber, A.Z. New Insights into Perfluorinated Sulfonic-Acid Ionomers. *Chem. Rev.* **2017**, *117*, 987–1104. [[CrossRef](#)]
84. Li, W.; Manthiram, A.; Guiver, M.D. Acid–base blend membranes consisting of sulfonated poly(ether ether ketone) and 5-amino-benzotriazole tethered polysulfone for DMFC. *J. Membr. Sci.* **2010**, *362*, 289–297. [[CrossRef](#)]
85. Ma, M.; Clark, E.L.; Therkildsen, K.T.; Dalsgaard, S.; Chorkendorff, I.; Seger, B. Insights into the carbon balance for CO₂ electroreduction on Cu using gas diffusion electrode reactor designs. *Energy Environ. Sci.* **2020**, *13*, 977–985. [[CrossRef](#)]
86. Lee, B.; Sakamoto, Y.; Hirabayashi, D.; Suzuki, K.; Hibino, T. Direct oxidation of methane to methanol over proton conductor/metal mixed catalysts. *J. Catal.* **2010**, *271*, 195–200. [[CrossRef](#)]
87. Santos, M.C.L.; Nunes, L.C.; Silva, L.M.G.; Ramos, A.S.; Fonseca, F.C.; de Souza, R.F.B.; Neto, A.O. Direct Alkaline Anion Exchange Membrane Fuel Cell to Converting Methane into Methanol. *ChemistrySelect* **2019**, *4*, 11430–11434. [[CrossRef](#)]
88. Nandenha, J.; Piasentin, R.M.; Silva, L.M.G.; Fontes, E.H.; Neto, A.O.; de Souza, R.F.B. Partial oxidation of methane and generation of electricity using a PEMFC. *Ionics* **2019**, *25*, 5077–5082. [[CrossRef](#)]
89. Rocha, R.S.; Camargo, L.M.; Lanza, M.R.V.; Bertazzoli, R. A Feasibility Study of the Electro-recycling of Greenhouse Gases: Design and Characterization of a (TiO₂/RuO₂)/PTFE Gas Diffusion Electrode for the Electrosynthesis of Methanol from Methane. *Electrocatalysis* **2010**, *1*, 224–229. [[CrossRef](#)]
90. Nandenha, J.; Fontes, E.H.; Piasentin, R.M.; Fonseca, F.C.; Neto, A.O. Direct oxidation of methane at low temperature using Pt/C, Pd/C, Pt/C–ATO and Pd/C–ATO electrocatalysts prepared by sodium borohydride reduction process. *J. Fuel Chem. Technol.* **2018**, *46*, 1137–1145. [[CrossRef](#)]
91. Nandenha, J.; Nagahama, I.H.F.; Yamashita, J.Y.; Fontes, E.H.; Ayoub, J.M.S.; de Souza, R.F.B.; Fonseca, F.C.; Neto, A.O. Activation of Methane on PdZn/C Electrocatalysts in an Acidic Electrolyte at Low Temperatures. *Int. J. Electrochem. Sci.* **2019**, *14*, 10819–10834. [[CrossRef](#)]
92. de Moura Souza, F.; de Souza, R.F.B.; Batista, B.L.; dos Santos, M.C.; Fonseca, F.C.; Neto, A.O.; Nandenha, J. Methane activation at low temperature in an acidic electrolyte using PdAu/C, PdCu/C, and PdTiO₂/C electrocatalysts for PEMFC. *Res. Chem. Intermed.* **2020**, *46*, 2481–2496. [[CrossRef](#)]
93. Fan, Q. Method for Producing Methanol from Methane. U.S. Patent 2014/0124381 A1, 20 October 2015.
94. Fan, Q. Non-Faradaic Electrochemical Promotion of Catalytic Methane Reforming for Methanol Production. U.S. Patent 9499917B2, 22 November 2016.
95. Garcia, L.M.S.; Rajak, S.; Chair, K.; Godoy, C.M.; Silva, A.J.; Gomes, P.V.R.; Sanches, E.A.; Ramos, A.S.; De Souza, R.F.B.; Duong, A.; et al. Conversion of Methane into Methanol Using the [6,6'-(2,2'-Bipyridine-6,6'-Diyl)bis(1,3,5-Triazine-2,4-Diamine)](Nitrate-O)Copper(II) Complex in a Solid Electrolyte Reactor Fuel Cell Type. *ACS Omega* **2020**, *5*, 16003–16009. [[CrossRef](#)]
96. Liu, F.; Yan, Y.; Chen, G.; Wang, D. Recent advances in ambient electrochemical methane conversion to oxygenates using metal oxide electrocatalysts. *Green Chem.* **2024**. Advance Article. [[CrossRef](#)]
97. Verma, S.; Lu, S.; Kenis, P.J.A. Co-electrolysis of CO₂ and glycerol as a pathway to carbon chemicals with improved techno-economics due to low electricity consumption. *Nat. Energy* **2019**, *4*, 466–474. [[CrossRef](#)]
98. Koolen, C.D.; Luo, W.; Züttel, A. From Single Crystal to Single Atom Catalysts: Structural Factors Influencing the Performance of Metal Catalysts for CO₂ Electroreduction. *ACS Catal.* **2023**, *13*, 948–973. [[CrossRef](#)]

99. Zhang, J.; Pham, T.H.M.; Ko, Y.; Li, M.; Yang, S.; Koolen, C.D.; Zhong, L.; Luo, W.; Züttel, A. Tandem effect of Ag@C@Cu catalysts enhances ethanol selectivity for electrochemical CO₂ reduction in flow reactors. *Cell Rep. Phys. Sci.* **2022**, *3*, 100949. [[CrossRef](#)]
100. Maiyalagan, T.; Saji, V.S. *Electrocatalysts for Low Temperature Fuel Cells: Fundamentals and Recent Trends*; John Wiley & Sons: Hoboken, NJ, USA, 2017.

Disclaimer/Publisher's Note: The statements, opinions and data contained in all publications are solely those of the individual author(s) and contributor(s) and not of MDPI and/or the editor(s). MDPI and/or the editor(s) disclaim responsibility for any injury to people or property resulting from any ideas, methods, instructions or products referred to in the content.